



## Review article

## Recent progress in TiO<sub>2</sub>-Based photocatalysts for conversion of CO<sub>2</sub> to hydrocarbon fuels: A systematic review

Md. Arif Hossen<sup>a,b</sup>, H.M. Solayman<sup>c</sup>, Kah Hon Leong<sup>d</sup>, Lan Ching Sim<sup>e</sup>, Nurashikin Yaacof<sup>c</sup>, Azrina Abd Aziz<sup>c,\*</sup>, Lihua Wu<sup>f</sup>, Minhaj Uddin Monir<sup>g</sup>

<sup>a</sup> Faculty of Chemical and Process Engineering Technology, Universiti Malaysia Pahang, 26300, Gambang, Pahang, Malaysia

<sup>b</sup> Center for Environmental Science & Engineering Research, Chittagong University of Engineering and Technology, 4349, Chattogram, Bangladesh

<sup>c</sup> Faculty of Civil Engineering Technology, Universiti Malaysia Pahang, 26300, Gambang, Pahang, Malaysia

<sup>d</sup> Department of Environmental Engineering, Faculty of Engineering and Green Technology, Universiti Tunku Abdul Rahman, 31900, Kampar, Perak, Malaysia

<sup>e</sup> Department of Chemical Engineering, Lee Kong Chian Faculty of Engineering and Science, Universiti Tunku Abdul Rahman, 43200, Kajang, Selangor, Malaysia

<sup>f</sup> Kuantan Sunny Scientific Collaboration Sdn. Bhd. Suites 7.23, 7th Floor, Imbi Plaza, Jalan Imbi, 55100, Kuala Lumpur, Malaysia

<sup>g</sup> Department of Petroleum and Mining Engineering, Jashore University of Science and Technology, 7408, Jashore, Bangladesh

## ARTICLE INFO

## Keywords:

TiO<sub>2</sub> photocatalyst  
CO<sub>2</sub> reduction  
Surface modification  
PRISMA method  
Hydrocarbon production

## ABSTRACT

Photocatalytic conversion of CO<sub>2</sub> by using sunlight and TiO<sub>2</sub> photocatalysts is a promising approach which produce hydrocarbon fuels to meet the future energy demands with hardly affecting the environment. This systematic review aims to provide rigorous overview of recent progress in TiO<sub>2</sub>-based CO<sub>2</sub> photoreduction to produce hydrocarbon fuels along with future challenges. Preferred Reporting Items for Systematic Reviews and Meta-Analyses (PRISMA) method was adopted to perform this systematic review. It uses explicit systematic approaches that are chosen to prevent bias, resulting in accurate data collection which helps to draw reliable conclusions. Peer-reviewed articles published in English language between year 2018–2022 were chosen from two main databases, namely Web of Science and Scopus. Depending on the search criteria 62 articles were selected for reviewing critically. Literature suggests that TiO<sub>2</sub>-based photocatalysts have been increasingly used for reducing CO<sub>2</sub> to hydrocarbon fuels. Morphological alterations and surface modification techniques have been widely utilized to improve the photocatalytic performance and minimize limitations of pure TiO<sub>2</sub>. Despite extensible efforts in this field, the utilization of hydrocarbon fuels still far away from practical applications. There are some challenges need to be addressed like environment friendly low-cost synthesis and modification method development, maximum visible light utilization, design of photoreactor with suitable product selectivity and kinetic model development for CO<sub>2</sub> reduction. This study portrays increased clarity regarding the advances and way forwards of crucial topics TiO<sub>2</sub>-based CO<sub>2</sub> photoreduction. Such systematic review is crucial for researchers and academicians for setting future planning.

### 1. Introduction

Energy crisis and air pollution scenario of the world getting severe in recent years due to the increasing fuel consumption rate and rapid industrialization [1–3]. The U.S. Energy Information Administration (EIA) has predicted that by 2050, global energy consumption may increase by 50% [4]. Around 80% of the global energy demand is still fulfilled by using fossil fuels [5,6]. The key factor contributing to global warming and increasing greenhouse gases is the excessive burning of fossil fuels [7,8]. According to the United States Environmental Protection Agency (USEPA), CO<sub>2</sub> emission contributes roughly 80% of all

greenhouse gas emissions, and 65% of those emissions come from burning fossil fuels [9]. The world is gradually shifting to renewable energy sources for energy consumption considering the steady increase of CO<sub>2</sub> emission from fossil fuels combustion. Between 2017 and 2021, oil consumption declined by 2.75% each year, respectively, while renewable energy consumption increased by 4.85% per year (Fig. 1).

Solar energy is the most prevalent of the various types of renewable energy sources. Research and development strategies are going on to produce hydrocarbon fuels from CO<sub>2</sub> using solar energy. Photocatalytic production of hydrocarbon fuels from CO<sub>2</sub> is a viable technique for tackling global environmental issues while also ensuring future energy

\* Corresponding author.

E-mail address: [azrinaaziz@ump.edu.my](mailto:azrinaaziz@ump.edu.my) (A. Abd Aziz).

<https://doi.org/10.1016/j.rineng.2022.100795>

Received 27 September 2022; Received in revised form 20 November 2022; Accepted 22 November 2022

Available online 24 November 2022

2590-1230/© 2022 The Authors. Published by Elsevier B.V. This is an open access article under the CC BY-NC-ND license (<http://creativecommons.org/licenses/by-nc-nd/4.0/>).

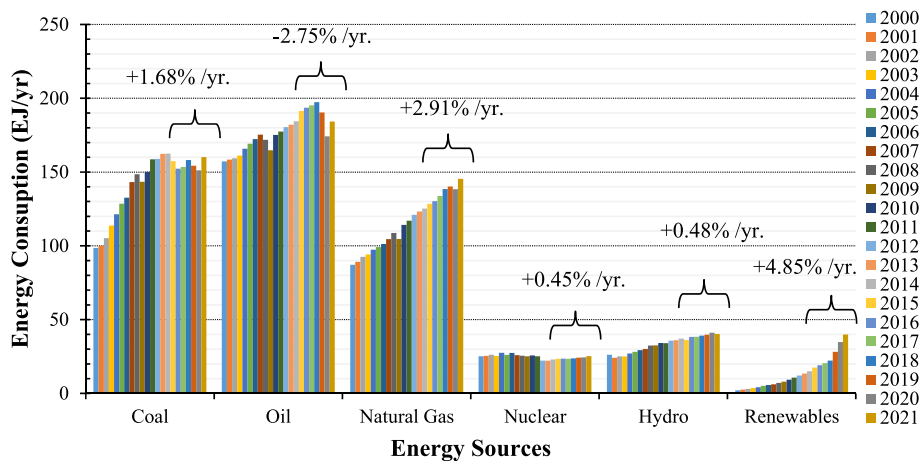


Fig. 1. Global energy consumption from various sources from 2000 to 2021 [10].

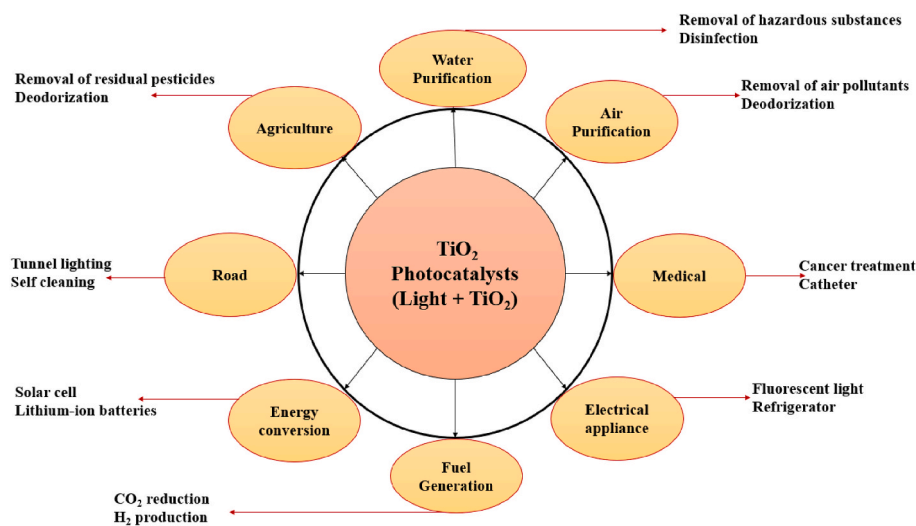


Fig. 2. Application of TiO<sub>2</sub>-based photocatalysts.

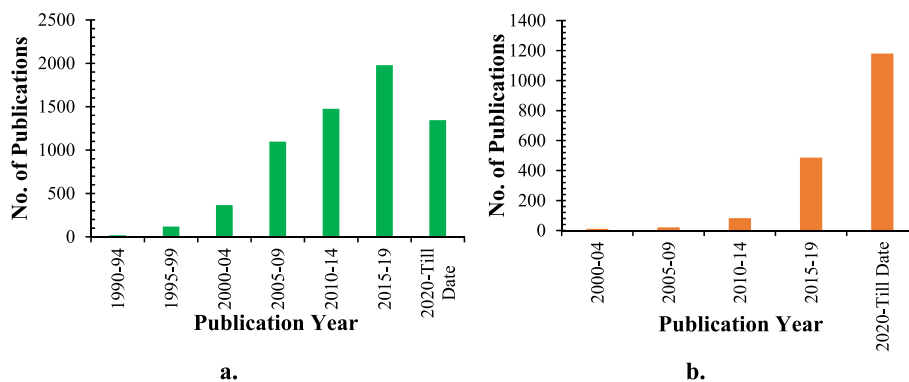


Fig. 3. Number of publications searching the terms: a) TiO<sub>2</sub> photocataly\* or titanium dioxide photocataly\*; and b) photocatalytic CO<sub>2</sub> reduction or photocatalytic CO<sub>2</sub> conversion or photocatalytic conversion of CO<sub>2</sub> or photocatalytic carbon dioxide reduction or photocatalytic carbon dioxide conversion or photocatalytic conversion of carbon dioxide. [Only journal articles (original and review) and conference papers included using Scopus database searched on November 15, 2022].

security [11]. Different semiconductor materials used as a photocatalyst in CO<sub>2</sub> photoreduction process. They are TiO<sub>2</sub>, Cu<sub>2</sub>O, ZnO, ZnS, CdTe CdS, CdSe, WO<sub>3</sub> and Bi<sub>2</sub>WO<sub>6</sub> [12–15]. TiO<sub>2</sub> is the most used photocatalyst for its availability, stability, photoactivity and low toxic material properties [16,17]. Along with fuel generation TiO<sub>2</sub> has diverse

applications, as shown in Fig. 2. Since the discovery of TiO<sub>2</sub> as a photocatalyst by Fujishima and Honda, it has perceived a lot of attention as a possibility for CO<sub>2</sub> photoreduction into hydrocarbon fuels. Fig. 3 depicts the growing rate of publications dealing with TiO<sub>2</sub> photocatalysts and CO<sub>2</sub> photoreduction. There is a huge increase in number of studies

**Table 1**  
Searching string used in this study and the total number of publications from two important databases.

Database	Searching String	Total	Combined
Scopus	TITLE-ABS-KEY (("TiO <sub>2</sub> " OR "Titanium Dioxide" OR "TiO <sub>2</sub> Photocataly*" OR "TiO <sub>2</sub> Semiconductor") AND ("CO <sub>2</sub> " OR "CO <sub>2</sub> Reduction" OR "Carbon Dioxide Reduction" OR "Reduction of Carbon Dioxide" OR "Conversion of CO <sub>2</sub> ") AND ("Photocatalytic CO <sub>2</sub> Reduction" OR "Photocatalytic Carbon Dioxide Reduction" OR "Photo-electrocatalytic Carbon Dioxide Reduction" OR "Photocatalytic Production of Solar Fuels" OR "Photocatalytic Production of Methane" OR "Carbon Dioxide to Methane" OR "CO <sub>2</sub> to CH <sub>4</sub> " OR "CO <sub>2</sub> to Hydrocarbon Fuels"))	337	853
Web of Science (WoS) core collection	TS= (("TiO <sub>2</sub> " OR "Titanium Dioxide" OR "TiO <sub>2</sub> Photocataly*" OR "TiO <sub>2</sub> Semiconductor") AND ("CO <sub>2</sub> " OR "CO <sub>2</sub> Reduction" OR "Carbon Dioxide Reduction" OR "Reduction of Carbon Dioxide" OR "Conversion of CO <sub>2</sub> ") AND ("Photocatalytic CO <sub>2</sub> Reduction" OR "Photocatalytic Carbon Dioxide Reduction" OR "Photo-electrocatalytic Carbon Dioxide Reduction" OR "Photocatalytic Production of Solar Fuels" OR "Photocatalytic Production of Methane" OR "Carbon Dioxide to Methane" OR "CO <sub>2</sub> to CH <sub>4</sub> " OR "CO <sub>2</sub> to Hydrocarbon Fuels"))	707	

Note: The data here includes reviewed and original articles of all languages.

considering photocatalytic CO<sub>2</sub> reduction in the last three years (Fig. 3b).

TiO<sub>2</sub> is the most affordable, readily useable, and well-characterized UV light active semiconductor photocatalyst. However, practical applications of TiO<sub>2</sub> are greatly hindered by its wide inherent band gap (E<sub>g</sub> = 3.2 eV for anatase), quick recombination of photogenerated charges, and low solar light utilization (about 5%) [18,19]. Therefore, considering practical standpoint, it is crucial to increase the capacity of TiO<sub>2</sub> for light absorption and electron-hole separation efficiency. Nevertheless, CO<sub>2</sub> is a highly stable molecule ( $\Delta G^\circ = -400 \text{ kJ mol}^{-1}$ ) with linear symmetrical configuration, fully oxidized carbon, and an average carbon-oxygen double bond energy of up to 804.4 kJ mol<sup>-1</sup> (at 298 K) [20]. Thus, strong photocatalyst is required to convert it into value-added chemicals. TiO<sub>2</sub> produces electron and holes when exposed to UV light, which aids in the dissociation of CO<sub>2</sub> bonds. The rate at which CO<sub>2</sub> breakdown will depend on how quickly electron-holes are generated. Improvement of charge separation efficiency and enhancement of visible light absorption can be attributed TiO<sub>2</sub> as strong photocatalyst to convert CO<sub>2</sub> [21]. Along with morphological modification, most widely used approaches to produce highly effective TiO<sub>2</sub> for CO<sub>2</sub> photoreduction is the modification of TiO<sub>2</sub> surface by using metal deposition, metal doping, non-metal doping, dispersion on supports, carbon-based materials doping, surface sensitization and heterojunction methods [22,23].

With increasing research investigating to improve CO<sub>2</sub> photoreduction performance of TiO<sub>2</sub>-based photocatalysts, summarizing those findings systematically is deemed crucial. Some descriptive review works on TiO<sub>2</sub>-based CO<sub>2</sub> photoreduction have been done [7,22,24], as far as our knowledge there is no systematic review performed. Systematic review offers a structured overview on a particular topic that aids academics and researchers in keeping updated with the literature [25]. The purpose of this paper is to systematically summarize the recent advances with future challenges of TiO<sub>2</sub>-based photocatalysts for conversion of CO<sub>2</sub> to hydrocarbon fuels. Particularly, various modification

techniques of TiO<sub>2</sub> to enhance CO<sub>2</sub> photoreduction are extensively discussed. Moreover, great importance is also given to providing deeper understanding on factors affecting the CO<sub>2</sub> photoreduction performance. Finally, future challenges and way forwards for practical applications of TiO<sub>2</sub> photocatalysts for CO<sub>2</sub> photoreduction are described.

## 2. Methods

This work was driven by investigating recent progress and future challenges of TiO<sub>2</sub>-based photocatalysts for photoreduction of CO<sub>2</sub> to hydrocarbon fuels. In order to fully understand the current progress and impending challenges we explored the recent literature as the primary source. Preferred Reporting Items for Systematic Reviews and Meta-Analyses (PRISMA), a well-known published protocol to perform a systematic literature review was used in this study. This method uses very clear and systematic approaches that are specifically chosen to avoid bias, resulting in accurate information gathering which leads to create trustworthy conclusions.

### 2.1. Literature search process

The present study was carried out utilizing two key databases, Scopus and Web of Science (WoS) along with other sources, because both databases are reliable and cover more than 256 areas of study, including environmental fields [26]. We formulated a search string based on our understanding and knowledge in relevant field. The search string used in this study tabulated in Table 1. The literature was searched using advanced search options in both databases. First, we queried both database in early June 2022 and second time on the November 15, 2022, for getting maximum publications in the year 2022. Fig. 4 depicts the general screening methods and the flow of identifying relevant publications for reviewing. In the identification stage 337 articles from Scopus, 707 articles from WoS database and 171 articles from other sources were retrieved. When researchers retrieve publications from two or more databases using the same library format, merging the articles from databases to undertake unique analyses might be difficult, particularly when the databases are large. In this study unique technique suggested by Echchakoui [27] to merge publications of all databases was used. In the screening process, total of 201, articles were excluded due to duplication in both databases. Inclusion and exclusion criteria were set to further refine the 1014 results obtained after removing replicate and merging both articles of both databases.

### 2.2. Eligibility criteria

We refined our results by only considering exclusion criteria: (i) review articles; (ii) book series & book chapter; (iii) conference proceedings; (iv) non-English language; (v) published before year 2018; (vi) meta-analysis & articles in press; and (vii) articles not open access & access by UMP library. After considering the articles based on inclusion and exclusion criteria, 102 studies remained in eligibility stage. A database with the 102 articles containing titles, abstracts and full texts was created in Mendeley reference management software. More importantly, at this step, all of the papers' titles, abstracts, and contents were carefully scrutinized to make sure they met the inclusion requirements and were appropriate for use in the current study in order to fulfil the objectives. Consequently, a total of 40 articles were excluded because they are not based on empirical data and focused on TiO<sub>2</sub>-based photoactivity. Finally, total 62 remaining articles were selected to analyze.

## 3. Results

### 3.1. Overview of the selected studies

Research on photocatalytic CO<sub>2</sub> reduction to produce hydrocarbon

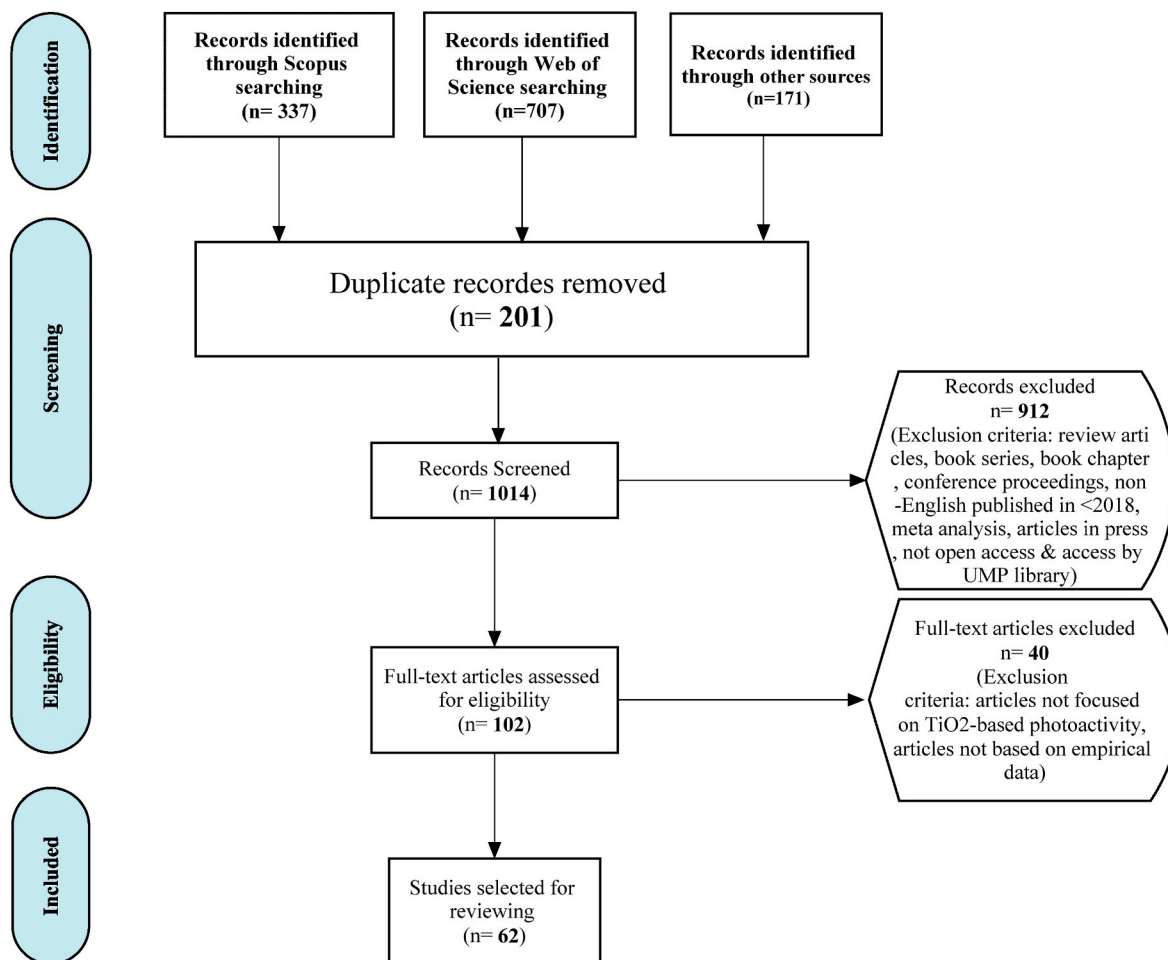


Fig. 4. Flowchart of study based on the PRISMA recommended protocol.

fuels using TiO<sub>2</sub>-based photocatalysts has been increasing for getting alternative options to reduce pressure on fossil fuels. In this review, 62 articles from 17 different countries of the world were selected based on the criteria depicted in Fig. 4. The largest number of studies were carried out in Asian region (Fig. 5a). The highest around 42% (n = 26) of studies reviewed were conducted in China (Fig. 5b). All articles selected for this study were published between 2018 and 2022. Fig. 5c exhibits year wise selected publications number. About 60% (n = 37) of studies reviewed were published between 2020 and 2021. The articles reviewed were obtained from 36 different journals including nine (09) publishers. Most of these journals were published in the subject areas of chemical engineering, materials science, environmental science, chemistry, and energy.

### 3.2. Recent progress of TiO<sub>2</sub>-based photocatalysis

Titanium dioxide (TiO<sub>2</sub>) is the most studied semiconductor photocatalysts, and it has been utilized remarkably in the field of environmental purification and energy generation. It is worth mentioning that almost two third of the recent publications on photocatalysis utilizing TiO<sub>2</sub> as a photocatalyst which shown in Fig. 6. When exposed to a photon with an energy equivalent to or more than its bandgap, TiO<sub>2</sub> can produce electron-hole pairs. Based on the specific electronic pathway maintained by a certain species, the disposition of photogenerated electrons ( $e_{CB}^-$ ) and holes ( $h_{VB}^+$ ) may be identified [28]. Typical reaction mechanism involved in photocatalytic processes and approach in CO<sub>2</sub> photoreduction is illustrated in Fig. 7a, b. The discharge of heat occurs when the input energy is depleted.

Generally, appropriate semiconductor is classified by three key characteristics: firstly, the bandgap energy ( $E_g$ ), secondly, the locations of conduction band (CB) and valence band (VB), and thirdly, the behaviors of photogenerated electrons and holes [28,31]. The rates of interface charge recombination and interfacial charge carrier are the important behaviors of photogenerated electrons and holes [32]. One of the fundamental barriers to the practical application of TiO<sub>2</sub> photocatalysts is charge recombination at deep level defects, which reduces TiO<sub>2</sub>'s photocatalytic performance [33–36]. Yu et al. [36] proposes a method that employs shallow-level defects thermally stimulating the migration of trapped electrons above the deep-level defects via solution plasma processing (SPP) technology. Semiconductor photocatalysts with  $E_g > 3.0$  eV, for example, are solely active in UV light, while those with  $E_g < 3.0$  eV are more effective in visible light. The band positions of mostly used semiconductors (such as TiO<sub>2</sub>, Cu<sub>2</sub>O, CdSe, ZnO, CdS, WO<sub>3</sub> and Bi<sub>2</sub>WO<sub>6</sub>) and redox potentials versus (vs.) Normal Hydrogen Electrode (NHE) of CO<sub>2</sub> reduction at pH = 7 are shown in Fig. 7c. The association between band energy and the redox potential of the product selectivity determines the types of compounds that can be created from the process [37]. The redox potential and band gap relationship also applies to CO<sub>2</sub> reduction to various hydrocarbon fuels, such as CH<sub>3</sub>OH, HCOOH, and CH<sub>4</sub>. Both TiO<sub>2</sub> and ZnO, which are widely used photocatalysts, have advantages and disadvantages. Use of TiO<sub>2</sub> instead of ZnO can be favorable in terms of bandgap, cost, stability, and many other characteristics. Since its discovery in 1972, researchers have been attempting to extract the photocatalytic benefits of TiO<sub>2</sub> as well as solutions to its drawbacks.



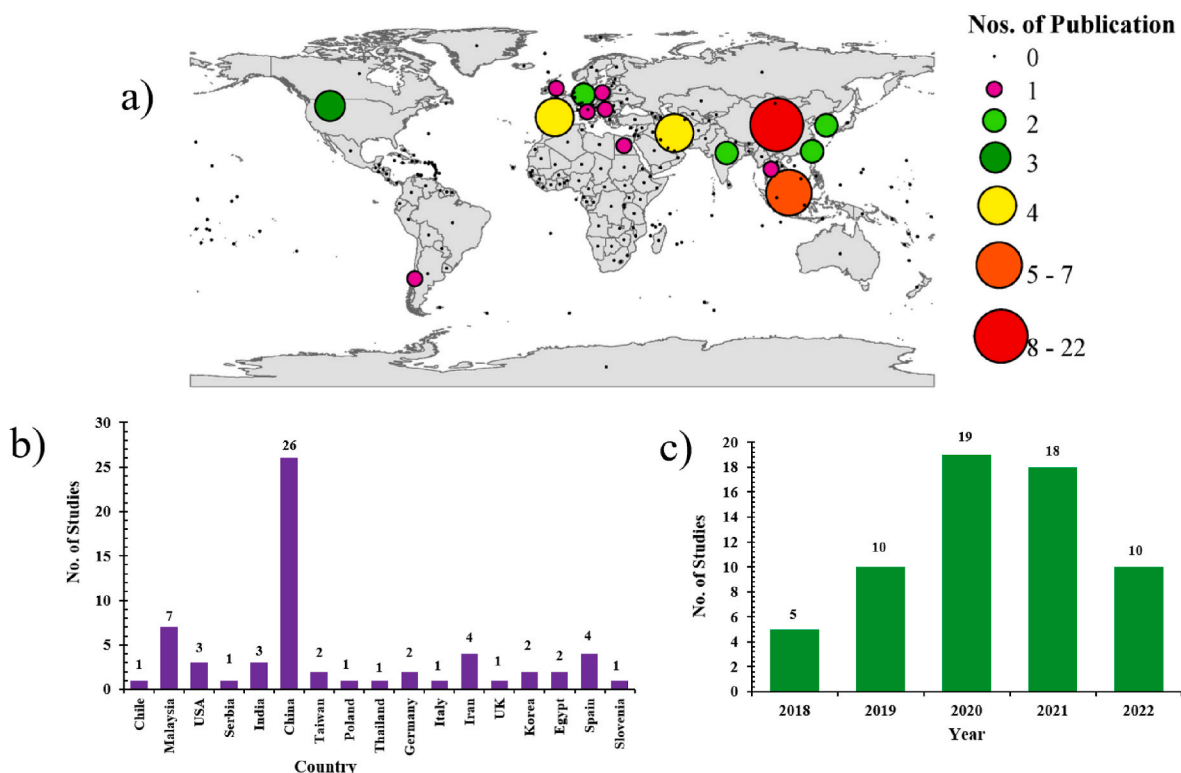


Fig. 5. Number of studies reviewed from specific countries: a) projected in the world map, b) projected in a bar chart and c) year-wise selected studies.

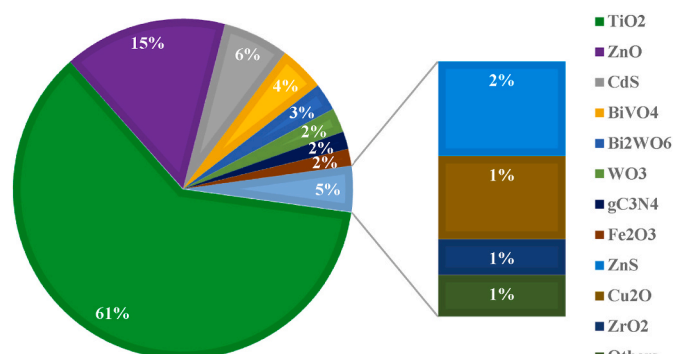


Fig. 6. Recent publications on photocatalysis utilizing different semiconductors from 2018 to 2022. (Publications search by using Scopus database).

### 3.3. Factors affecting the photocatalytic activity of TiO<sub>2</sub>-based photocatalysts

#### 3.3.1. Particle size and shape of the photocatalysts

The photocatalytic performance of a catalyst is comprehensively affected by the particle size and shape of the catalyst because a catalyst with small particle size and desired shape holds sufficient surface-active sites and there is a more possibility to promote the interfacial charge separation [31]. The synthesis methods of photocatalysts have significant influences on their morphology [38]. Sol-gel, template assisted synthesis, hydrothermal treatment and electrochemical anodization are frequently used methods for the synthesis of TiO<sub>2</sub> nanostructures. Among these methods electrochemical anodization allows for the development of self-organized TiO<sub>2</sub> nanostructures with low cost and simplicity of geometry control (length, diameter, and wall thickness) by the use of appropriate anodization parameters [39]. It has been revealed that TiO<sub>2</sub> nanoparticles showed better photocatalytic performance than that of TiO<sub>2</sub> microparticles, which can be attributed to their smaller

diameter [40]. The travel distance required for photogenerated charge carriers are shortened when particle size decreases, hence, lowering charge recombination. Li et al. [41] investigated the consequences of particle size on the morphology and photocatalytic activity by alkali treated TiO<sub>2</sub>. By varying the alkali-hydrothermal duration (0–48 h), TiO<sub>2</sub> nanoparticles with various crystalline sizes were produced by them. Among the prepared samples, pore volume of TiO<sub>2</sub>-24 was found maximum with minimum pore diameter. The XPS spectrum of TiO<sub>2</sub>-X showed TiO<sub>2</sub>-24 had lower intensity versus binding energy curve. TiO<sub>2</sub>-24 nanoparticles exhibited better photocatalytic performance under visible light was due to the collective impacts of surfaces defects and crystalline size.

The morphology (shape) of nanoparticles has also influenced on the improvement of photocatalytic performance. The electron-hole recombination in nanotube (NT) shaped photocatalyst is greatly retarded because photogenerated electrons need to travel vectorially along the NT wall. For instance, Huang et al. [42] constructed one dimensional TiO<sub>2</sub> nanostructures through a single-step hydrothermal method. Results revealed that one dimensional (1D) TiO<sub>2</sub> nanostructures catalysts had a high specific surface area, improved photocatalytic CO<sub>2</sub> reduction. Methane was produced at highest yields of 19.16 and 12.71 μmol/g over the TiO<sub>2</sub> nanotubes (TNT) and nanorods (TNR), respectively, which were approximately 2.33 and 1.48 times higher than TiO<sub>2</sub> nanoparticles (TNP). The effect of facet on TiO<sub>2</sub> nanostructures and their photocatalytic performance was investigated by Kowalkińska et al. [43]. They noted that TiO<sub>2</sub> with octahedra exposing {101} facets had the maximum photoactivity and mineralization efficiency when exposed to UV-vis light, with these properties decreasing as subsequent facets develop and are exposed more.

#### 3.3.2. Surface area of the photocatalysts

Besides, morphology (shape, size) control of TiO<sub>2</sub>, the increase of specific surface area is another promising approach to achieve photocatalytic activity improvement. The surface area of nanoparticles depends on their porosity and particle size [44]. One dimensional TiO<sub>2</sub>

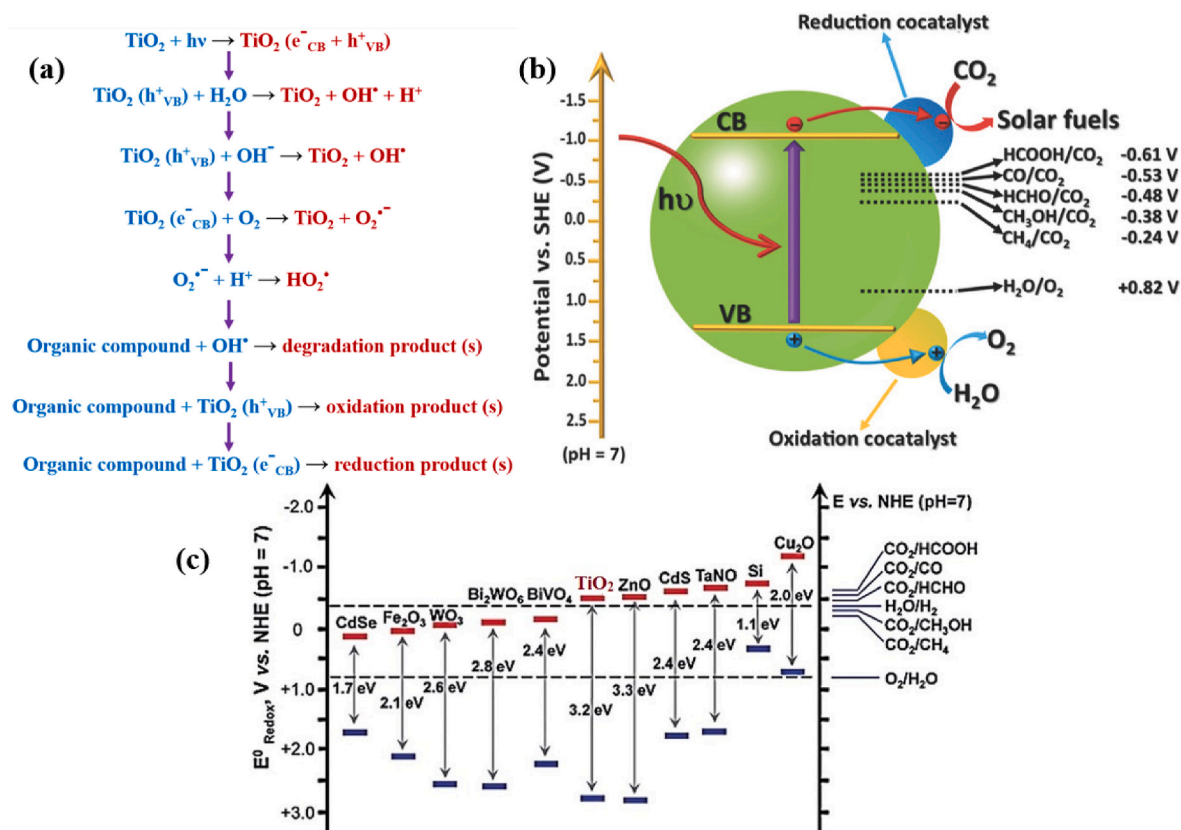


Fig. 7. (a) Mechanism involved in photocatalytic process (b) Typical approach in CO<sub>2</sub> photoreduction and (c) Band positions of certain semiconductors in relation to CO<sub>2</sub> reduction energy levels (Reproduced from Refs. [28,29,30] with permission).

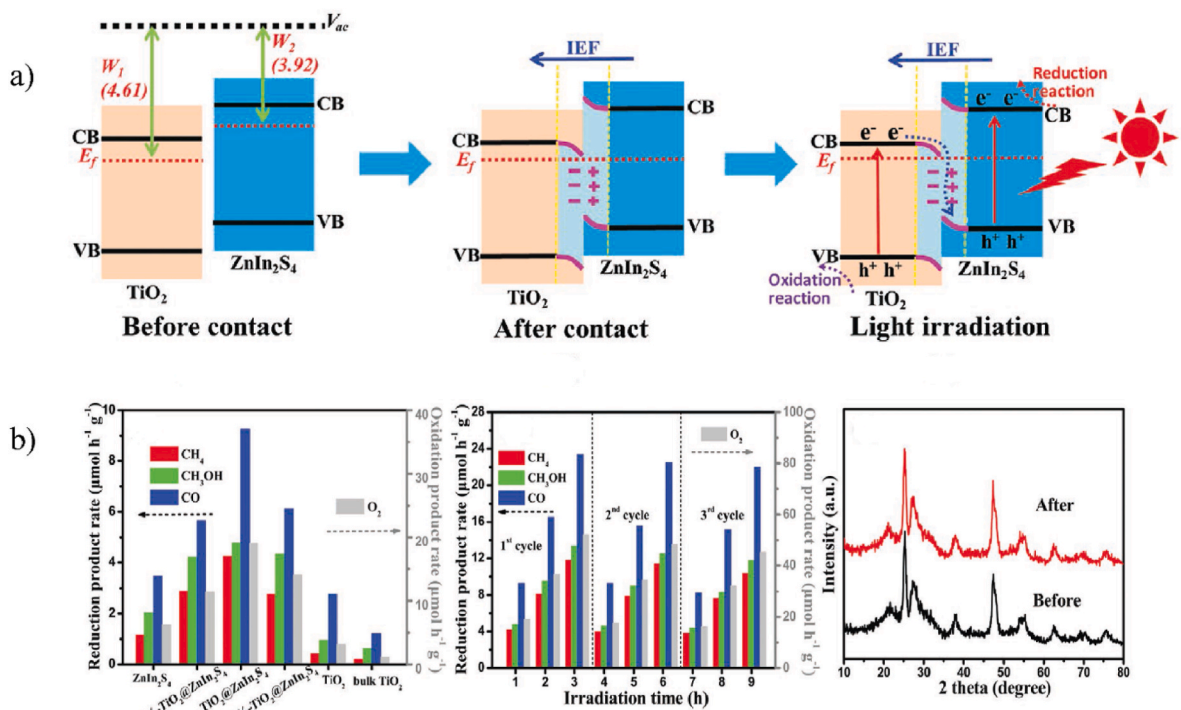
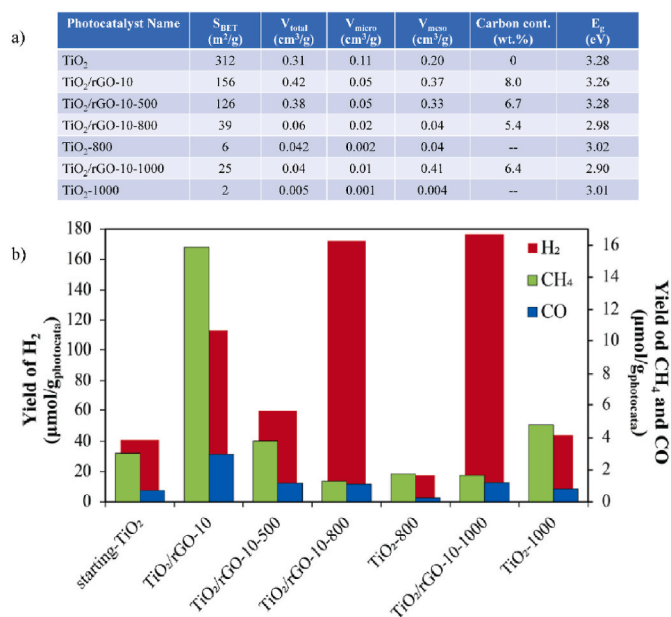


Fig. 8. Influence of specific surface area on enhancement of photocatalytic CO<sub>2</sub> reduction (a) illustration of the S-scheme transfer process between TiO<sub>2</sub> and ZnIn<sub>2</sub>S<sub>4</sub> and (b) Yield of products in photocatalytic CO<sub>2</sub> reduction (PCR) reaction of different samples with stability tests (Adopted from Ref. [47] with prior permission from Wiley Publisher).



**Fig. 9.** Effect of calcination temperature (a) properties of photocatalysts and (b) products yield of tested photocatalysts during CO<sub>2</sub> photoreduction with H<sub>2</sub>O (Reproduced from Ref. [50] with due permission from Elsevier).

nanostructures, especially, TNT has a high specific surface area and higher rate of photocatalytic CO<sub>2</sub> reduction ability than other nanostructures [42]. Due to the tubular shape and length, TNT intrinsically offer a high surface area [45]. Das et al. [46] explored a hierarchical ZnO–TiO<sub>2</sub> heterojunction strategy-driven technique to enhance photocatalytic performance by combining enhanced surface area and interfacial charge carrier. They reported that combining structural tuning with heterojunction leads to enhanced surface area and useful charge carrier separation, which improves photocatalytic activity. Wang et al. [47] investigated S-Scheme TiO<sub>2</sub>@ZnIn<sub>2</sub>S<sub>4</sub> photocatalyst for successful CO<sub>2</sub> photoreduction as shown in Fig. 8. The results indicated that improvement of photocatalytic CO<sub>2</sub> reduction is ascribed to the enlarge specific surface areas with sufficient active sites. When the TiO<sub>2</sub>@ZnIn<sub>2</sub>S<sub>4</sub> heterojunction is subjected to light, electrons are excited and easily move to the VB of ZnIn<sub>2</sub>S<sub>4</sub> and recombine with the photo-generated holes of ZnIn<sub>2</sub>S<sub>4</sub> due to the interface band bending and Coulomb interaction (Fig. 8a). As illustrated in Fig. 8b, the main photoreduction products of samples are CO, CH<sub>3</sub>OH, and CH<sub>4</sub>. In particular, when compared to pristine ZnIn<sub>2</sub>S<sub>4</sub> and TiO<sub>2</sub>, the overall CO<sub>2</sub> photoreduction conversion rates of the examined S-Scheme TiO<sub>2</sub>@ZnIn<sub>2</sub>S<sub>4</sub> photocatalyst enhanced by 2.75 and 4.43 times, respectively, reaching 18.32 μmol h<sup>-1</sup> g<sup>-1</sup>.

### 3.3.3. Calcination temperature

Calcination refers to the process of heating a material to a high temperature that is lower than the melting point. It significantly affects the produced photocatalysts' morphology, crystallinity, surface area, pore-volume, and phase structure, which influences the photocatalytic performance as well. Wu et al. [48] decorated Pd-calcined black TiO<sub>2</sub> nanoparticles in an argon environment using the sol-gel method. At various calcination temperatures, the synthesized photocatalyst was examined, and the maximum behavior was recorded photocatalyst calcined at 400 °C. In another study, Phromma et al. [49] investigated particle size, crystallite size, and phase separation of TiO<sub>2</sub> nanoparticles to determine the impact of calcination temperature on photocatalytic activity. The results showed that anatase had a significant impact on photocatalytic activity between 300 and 600 °C, however the particle size of TiO<sub>2</sub> was shown to have a dominant impact between 600 and 700 °C. Morawski et al. [50] examined the effect of

calcination temperature on TiO<sub>2</sub>/rGO for the CO<sub>2</sub> photoreduction. Above 500 °C calcined temperature substantial reduction of band gap energy and BET surface area was observed (Fig. 9a). This is due to the aggregation of TiO<sub>2</sub> particles during calcination and incorporation of rGO in composite. The highest yield for CH<sub>4</sub> and CO production was observed for TiO<sub>2</sub>/rGO-10 without calcination, followed by H<sub>2</sub> calcined at 1000 °C (Fig. 9b).

### 3.3.4. Photocatalytic reactors

The efficiency of photocatalytic CO<sub>2</sub> reduction is substantially influenced by the photocatalytic reactors utilized [51]. In most cases, CO<sub>2</sub> photoreduction is performed in either batch or continuous-flow mode reactor systems. For the case of batch type reactors, product accumulation and re-adsorption, as well as additional reverse or side reactions, are always a possibility [11]. Overall, batch type reactors are not a suitable choice for long-term or large-scale applications. Alternatively, continuous-flow type reactor systems can improve the aforementioned issues in batch type reactors [52]. Dilla et al. [53] constructed a tubular continuous flow reactor to improve the interaction between gaseous CO<sub>2</sub> reactants and the TiO<sub>2</sub> photocatalyst surface, allowing the approach to be used on a larger scale and in industrial application.

It is indispensable to ensure that the photocatalyst is illuminated to its maximum extent and comprehensive interaction of reactants occurs with the photocatalyst surface. In general, this entails two approaches: increasing the catalyst surface area and increasing the quantity of light incident on the reactor. A monolith photoreactor was constructed on a continuous photocatalytic reactor by Tahir [54] after loading the TiO<sub>2</sub> photocatalyst over structured 3D MAX Ti<sub>3</sub>AlC<sub>2</sub>. The higher yield rate of CO, H<sub>2</sub> and C<sub>2</sub>H<sub>6</sub> with good stability was observed using the monolith photoreactor in comparison with the fixed bed photoreactor (Fig. 10). Higher photocatalytic conversion rate was reported due to the lighted surface area to volume of the monolith photoreactor, high flow rates, decreased pressure drop, increased catalyst loading, and efficient exploitation of photon energy. Giusi et al. [55] developed a unique gas progression photocatalytic reactor relying on copper-functionalized nanomembranes for CO<sub>2</sub> photoreduction. They used a concept that was substantially distinct from traditional photocatalytic methods. It was possible to demonstrate for the first time the extremely selective CO<sub>2</sub> conversion to C1–C2 carboxylic acids without production of H<sub>2</sub>, CO, CH<sub>4</sub>, or other hydrocarbons due to the unique properties and conditions of the photoreactor.

## 3.4. Modification techniques to enhance the photocatalytic CO<sub>2</sub> reduction

TiO<sub>2</sub> photocatalysts received noteworthy attention in the field of CO<sub>2</sub> reduction reactions as they are readily available, affordable, stable, and environmentally safe. However, the two key problems preventing practical use are the restricted ability to absorb in the visible light spectrum and the quick recombination of photogenerated electrons and holes [56,57]. Through surface modifications, the properties of photocatalytic materials can be changed significantly, which provides the possibility to improve photocatalytic activity and even induces new photocatalytic reaction paths. In this section, the latest research progress of surface modifications techniques to improve the CO<sub>2</sub> photoreduction performance will be discussed. Several surface modification strategies as shown in Fig. 11 have been used overcome the drawbacks of TiO<sub>2</sub> and enhancing the CO<sub>2</sub> photoreduction.

### 3.4.1. Metal deposition

Metal deposition is an appealing approach to enhance the photocatalytic activity of TiO<sub>2</sub> nanocomposites. Although metal deposition is an expensive modification method, it significantly enhances electron–hole separation in semiconductor materials [22]. The ability of metals to accept photogenerated electrons improves as the working functionality of the metal increases. Consequently, it improves the electron–hole



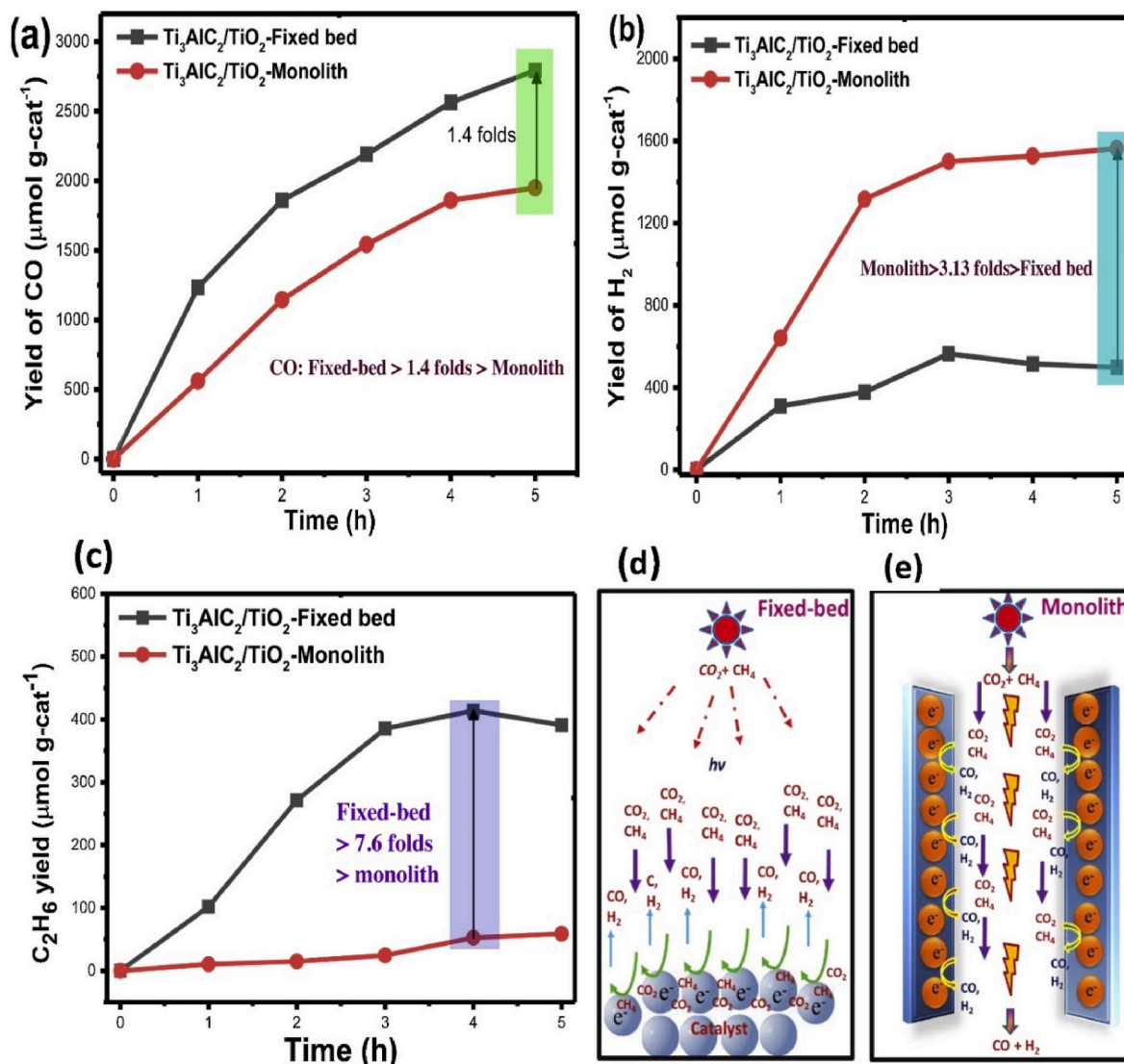


Fig. 10. Evaluation of  $\text{CO}_2$  photoreduction activity of fixed bed and monolith type photoreactor: (a) production of CO; (b) production of  $\text{H}_2$ ; (c) production of  $\text{C}_2\text{H}_6$ ; (d) process of fixed bed type reactor and (e) process of monolith type photoreactor system (Adopted from Ref. [54] with permission from Elsevier).

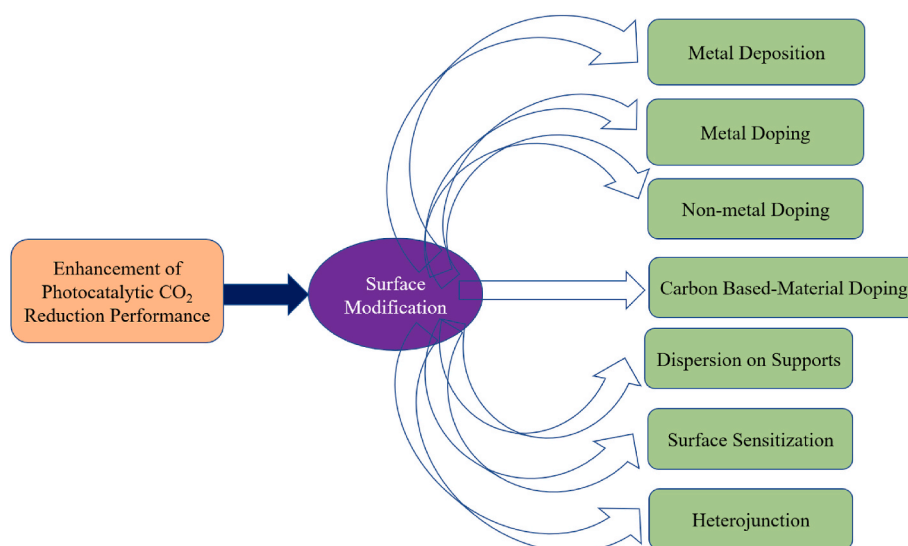


Fig. 11. Modification techniques to improve the  $\text{CO}_2$  photoreduction performance.

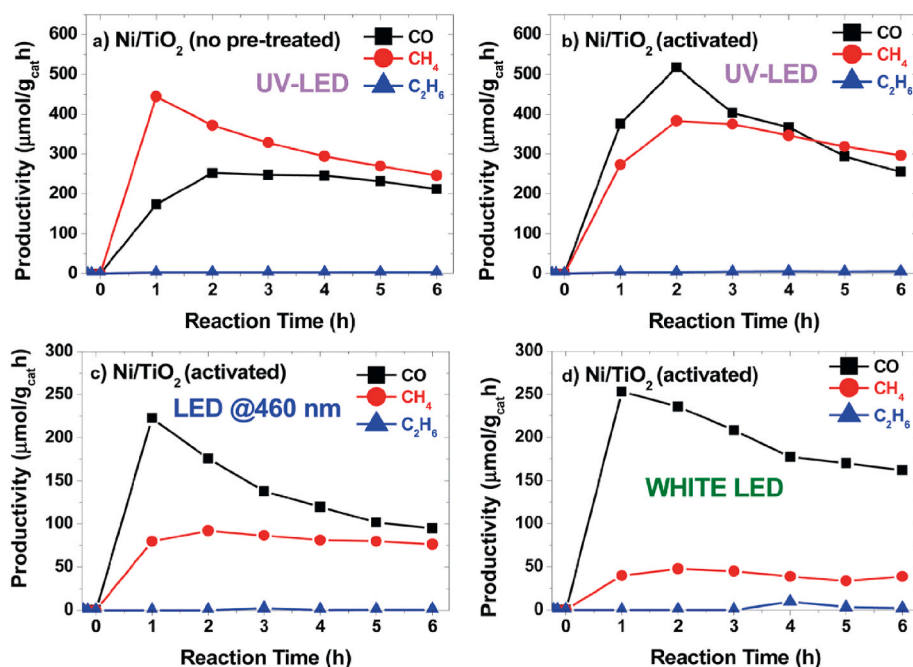


Fig. 12. Productivity of different products for Ni/TiO<sub>2</sub> catalyst under LED light irradiation (a) at 365 nm untreated, (b) at 365 nm activated, (c) at 460 nm and (d) white light (Adopted from Ref. [60] with permission from Royal Society of Chemistry).

separation, hence enhances the overall photocatalytic performance of TiO<sub>2</sub>. The absorption edge of TiO<sub>2</sub> is reduced when low bandgap energy metals are deposited, adjusting the visible light response [7]. Platinum (Pt), palladium (Pd), copper (Cu), nickel (Ni), gold (Au), and silver (Ag) are some of the most typically deposited metals. Devi et al. [58] used Pt-coated GO wrapped TNTs to increase CH<sub>4</sub> production by CO<sub>2</sub> photoreduction at a moderate temperature and pressure. They have successfully produced CH<sub>4</sub> at a high rate of 3.42 mmol g<sup>-1</sup> h<sup>-1</sup>. Reñones et al. [59] performed a study on Au–Ag deposited TiO<sub>2</sub> photocatalysts for CO<sub>2</sub> reduction. Compared to only producing syngas over pure TiO<sub>2</sub>, the results showed that bimetallic catalysts can alter the reaction selectivity into CH<sub>4</sub> under UV light irradiation. Sanz-Marco et al. [60] examined Ni deposited LED-driven TiO<sub>2</sub> for visible-light expanded conversion of CO<sub>2</sub>. The photocatalytic conversion of CO<sub>2</sub> into CO, CH<sub>4</sub> and C<sub>2</sub>H<sub>6</sub> alkanes was examined under LED irradiation at different wavelengths (Fig. 12). Results showed that when Ni/TiO<sub>2</sub> catalysts were illuminated at 365 nm, maximal productivity of CH<sub>4</sub> was 450 mmol g<sup>-1</sup> h<sup>-1</sup> and CO was 250 mmol g<sup>-1</sup> h<sup>-1</sup>, with C<sub>2</sub>H<sub>6</sub> production being nearly constant throughout the process, reaching roughly 2 mmol g<sup>-1</sup> h<sup>-1</sup>. Under the visible region of the solar spectrum the productivity of CO increased significantly compared to CH<sub>4</sub> and C<sub>2</sub>H<sub>6</sub> (Fig. 12c and d). Liu et al. [61] studied the performance of CO<sub>2</sub> photoreduction by implying Cu deposition on different TiO<sub>2</sub> substrates. It was revealed that both

TiO<sub>2</sub>@Cu and H–TiO<sub>2</sub>@Cu showed exceptional improvement for CO and CH<sub>4</sub> production. Another important finding was also found from the study that not only synthesis technique significantly enhances the CO<sub>2</sub> reduction activity after Cu deposition, however the substrate utilized for loading and the chemical state of inserted material will also affect the following catalytic activity. Recently, Zhan et al. [62] examined Pd nanoparticles on surface of TiO<sub>2</sub> for enhancing photocatalytic reduction of CO<sub>2</sub> to CH<sub>4</sub>. The Pd–HN–TiO<sub>2</sub> composite, which contains Pd, was synthesized by coordinating Pd(OAc)<sub>2</sub> with *N*-heterocyclic carbene in the skeleton, while HN serving as a platform to link TiO<sub>2</sub> with extensively dispersed Pd nanoparticles and increase CO<sub>2</sub> adsorption. Results showed that with a progress rate of 237.4 mol g<sup>-1</sup> h<sup>-1</sup> and selectivity of more than 99.9%, this composite with a surface area of 373 m<sup>2</sup> g<sup>-1</sup> improves CO<sub>2</sub> photoreduction efficiency to CH<sub>4</sub>. Pure TiO<sub>2</sub>, HN had a low CO<sub>2</sub> reduction efficiency for CH<sub>4</sub> and CO production, however the evolution rate of CH<sub>4</sub> increased somewhat after loading with Pd, while the rate of CO remained almost constant.

The visible-light activity of various semiconductor materials has been reported to be improved by Au and Ag nanoparticles deposition due to the effects of localized surface plasmon resonance (LSPR) and Schottky barrier development. With regard to the LSPR, an electromagnetic field is developed, and the photoreaction is enhanced through scattered photons, plasmonic energy transfer and electron excitation

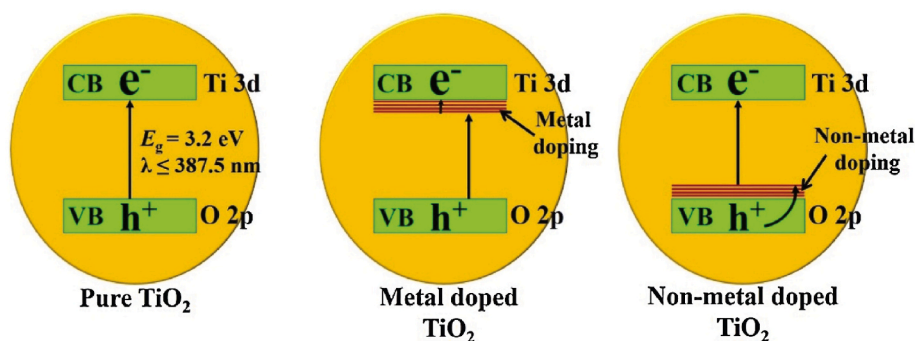


Fig. 13. Schematic illustration of band structure of the pure, metal doped and non-metal doped TiO<sub>2</sub> (Adopted from Ref. [68] with permission from Elsevier).



**Table 2**  
Summary of recent photocatalytic CO<sub>2</sub> reductions using metal doping.

Photocatalyst	Reductant	Photoreactor	Type of light	Product	Yield ( $\mu\text{mol g}^{-1} \text{h}^{-1}$ )	References
Pt-Ru/TiO <sub>2</sub>	CO <sub>2</sub> +H <sub>2</sub> O	Gas-closed circulation system	Xe lamp (320–780 nm)	CH <sub>4</sub>	38.7	[69]
Fe/TiO <sub>2</sub>	CO <sub>2</sub> + H <sub>2</sub>	Continuous flow quartz	Hg lamp (252 nm)	CO	166	[70]
Ag/TiO <sub>2</sub>	CO <sub>2</sub> +H <sub>2</sub> O	Continuous flow reactor	Xe lamp (365 nm)	CH <sub>4</sub>	0.42	[71]
				C <sub>2</sub> H <sub>6</sub>	0.10	
				CH <sub>3</sub> OH	1.9	
Ni-Bi/TiO <sub>2</sub>	CO <sub>2</sub> +H <sub>2</sub> O	Batch photo-reactor	Hg lamp (350 nm)	CH <sub>4</sub>	2.4	[67]
Cu/Cu+@TiO <sub>2</sub>	CO <sub>2</sub> + Na <sub>2</sub> SO <sub>4</sub>	Quartz	Xe lamp (350 nm)	CH <sub>4</sub>	21.1	[72]
Ag/TiO <sub>2</sub>	NaHCO <sub>3</sub> + H <sub>2</sub> O	Photochemical reactor	Hg lamp (350 nm)	CO	1.9	[73]
				CO	11.5	
				C <sub>2</sub> H <sub>6</sub>	28.8	
Pt-Au/R-TNTs	CO <sub>2</sub> +H <sub>2</sub> O	Quartz cell	LED light source (365 nm)	C <sub>2</sub> H <sub>6</sub>	28.8	[74]
Pd/TiO <sub>2</sub> -N	CO <sub>2</sub> + NaHCO <sub>3</sub>	Quartz cell	Hg lamp (320–390 nm)	CH <sub>4</sub>	360.0	[75]
				C <sub>2</sub> H <sub>4</sub>	9.2	
Pt/TiO <sub>2</sub> -N	CO <sub>2</sub> +H <sub>2</sub> O	Continuous flow reactor	LED light (365–530 nm)	CO	8.3	[76]
Au/TiO <sub>2</sub> (Ar)					8.8	
Ru-TiO <sub>2-x</sub>	NaHCO <sub>3</sub> + H <sub>2</sub> O vapor	Glass	Xe lamp (320 nm)	CH <sub>4</sub>	3.9	[77]
				C <sub>2</sub> H <sub>6</sub>	0.87	
				CH <sub>4</sub>	31.6	
		Reactor				

[63]. However, the development of a Schottky barrier increases photoactivity by trapping and extending the lifetime of the electrons. Khatun et al. [64] deposited Au nanoparticles in the TiO<sub>2</sub> nanotube by simple electrochemical deposition method to improve CO<sub>2</sub> photoreduction to CH<sub>4</sub>. Light harvesting properties of prepared Au-TNTs showed improvement under visible light owing to its LSPR behavior. The photocatalytic performance of TNTs and Au-TNTs increased considerably, yielding of 8.26% and 14.67% higher CH<sub>4</sub> production than bare TiO<sub>2</sub>, respectively. In another study, Feng et al. [63] demonstrated the photo-deposited Ag nanoparticles at two orders: MgO deposition followed by Ag (Ag/MgO/TiO<sub>2</sub>) and Ag deposition followed by MgO (MgO/Ag/TiO<sub>2</sub>) to improve the performance of CO<sub>2</sub> photoreduction. They revealed that the Ag/MgO/TiO<sub>2</sub> catalyst with seven deposited atomic layers of MgO and 5% Ag was 14-fold more active compared to pure TiO<sub>2</sub> for CO and CH<sub>4</sub> production. Li et al. [65] studied the photo-thermal catalytic performance of TiO<sub>2-x</sub>/CoO<sub>x</sub> photocatalysts for enhancing CO<sub>2</sub> photoreduction. The demonstrated 175 times yield of CH<sub>4</sub> than bare TiO<sub>2</sub> under UV irradiation at elevated temperature.

### 3.4.2. Metal doping

Metal doping is the most extensively used surface modification approach for preventing photogenerated electron-hole pairs from recombining on TiO<sub>2</sub> surface [22,66]. Pure TiO<sub>2</sub> is not able to absorb high photon energy due to its high band gap energy (3.2 eV), however doping reduces the band gap energy (Fig. 13). The addition of metal nanoparticles in the TiO<sub>2</sub> matrix causes structural defects and decreases the TiO<sub>2</sub> bandgap, lowering the absorption threshold to visible levels [22]. Nematollahi et al. [67] reported that incorporation of Ni and Bi gradually decreased band gap energy compared to pristine TiO<sub>2</sub> from 3.1 to 2.84 eV. Ni-Bi doped TiO<sub>2</sub> exhibited 6.5-fold more yield of CH<sub>4</sub> compared to pristine TiO<sub>2</sub>. In diverse investigations, Pt, Au, Ag, Fe, Cu, Ni, Pd, and Ru have been doped in TiO<sub>2</sub> matrix and shown to enhance its photocatalytic performance (Table 2).

In the case of a doped photocatalyst, photoreduction of CO<sub>2</sub> occurs on the surface of doped metal atoms. When photoexcitation happens, electrons are transmitted to the conduction band from valence band, subsequently these electrons are again moved to the metal heteroatom,

resulting in CO<sub>2</sub> conversion. Pan et al. [74] examined a binary component catalyst composed of single atoms (SAs- Pt and Au) which fixed on self-doped TNTs for CO<sub>2</sub> photoreduction. The results showed that the covalent interactions enabled an effective transfer of photogenerated electrons from the defect sites to the SAs, thereby improving separation of electron-holes and transfer of charge carrier. The maximum photocatalytic performance of Pt-Au/R-TNTs with 0.33 wt% single atom metals was recorded 149 times that of unmodified R-TNT, with yields of CH<sub>4</sub> and C<sub>2</sub>H<sub>6</sub> attained to 360.0 and 28.8  $\mu\text{mol g}^{-1} \text{h}^{-1}$ , respectively. Table 2 provided information on several metal-doped TiO<sub>2</sub>-based photocatalysts, associated experimental conditions, and CO<sub>2</sub> photoreduction performance. It is observed from the Table 2, the yield of CO<sub>2</sub> converted products is highly dependent on metal selection, reductant employed, photoreactor, source and intensity of light irradiation, and product selectivity. Tahir [70] investigated the performance of structured montmorillonite (MMT)-loaded Fe-doped TiO<sub>2</sub> (Fe/TiO<sub>2</sub>) nanocomposite for dynamic photoinduced CO<sub>2</sub> reduction to fuels using H<sub>2</sub> as the reductant. The results of the study showed that the photoactivity and stability of the Fe-MMT/TiO<sub>2</sub> catalyst for the generation of hydrocarbon fuels using the monolithic photoreactor was significantly enhanced in comparison to the cell-type reactor. Jin et al. [75] reported how to choose the appropriate metal cocatalysts in combination with TiO<sub>2</sub>'s surface basicity to improve photocatalytic CO<sub>2</sub> reduction efficiency. Uniform ligand-free metal nanoparticles of Ag, Cu, Au, Pd, and Pt doped on TiO<sub>2</sub> surfaces were investigated for CO<sub>2</sub> photoreduction utilizing water as the reductant. According to reported results, Ag is most active in producing CO, although Pd and Pt primarily generate hydrocarbons like methane and ethane, and amine-modified TiO<sub>2</sub> has a 2.4-fold enhancement in CO<sub>2</sub> photoreduction performance compared to TiO<sub>2</sub> without amines. Recently, Zhou et al. [77] investigated the performance of CO<sub>2</sub> photoreduction into CH<sub>4</sub> over Ru-doped TiO<sub>2</sub>. Improvement of CO<sub>2</sub> photoreduction to CH<sub>4</sub> was aided by the synergistic influence of Ru and oxygen vacancies. The optimum Ru-doped TiO<sub>2</sub> (1% Ru-TiO<sub>2-x</sub>) showed a substantial increase in photocatalytic activity, which is much greater than Ru-TiO<sub>2</sub> and TiO<sub>2-x</sub>, with a CH<sub>4</sub> yield of 31.6  $\mu\text{mol g}^{-1} \text{h}^{-1}$ .

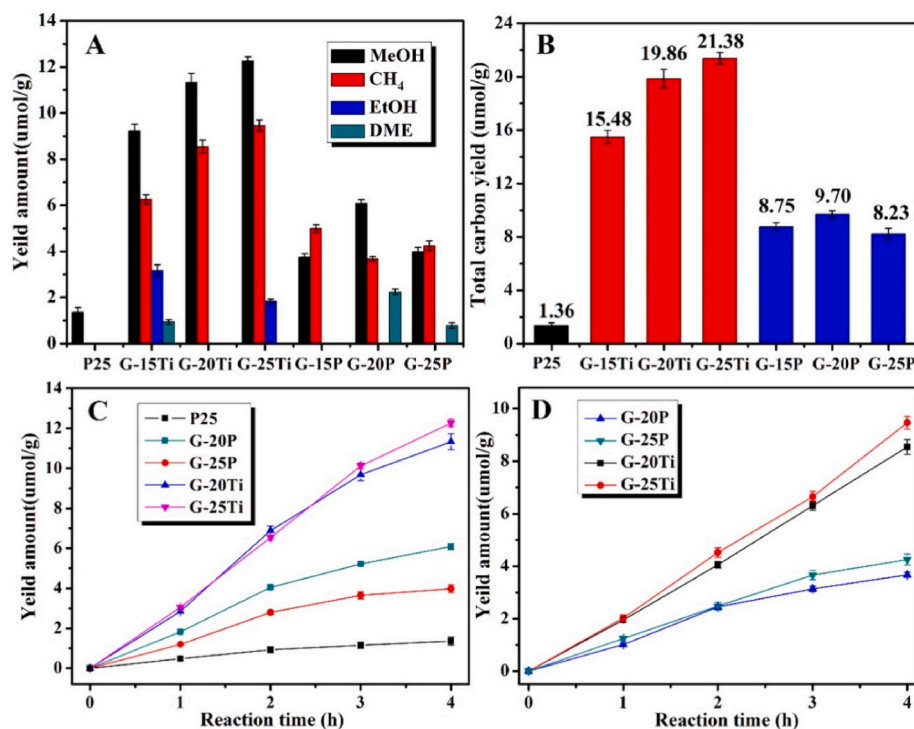


Fig. 14. Effects of reduced graphene oxide modified TiO<sub>2</sub> composites on photocatalytic CO<sub>2</sub> reduction (a) yields of MeOH, CH<sub>4</sub>, EtOH, and DME; (b) total carbon yields of CO<sub>2</sub> photoreduction for distinct catalysts; (c) yields rate of MeOH and (d) CH<sub>4</sub> (Taken from Ref. [90] with permission Elsevier).

### 3.4.3. Non-metal doping

Another type of surface modification approach of TiO<sub>2</sub> is non-metals doping. Non-metal doping has been used to improve the spectrum sensitivity of TiO<sub>2</sub> composites in a similar way to metal doping. As illustrated in Fig. 13, non-metals dopants lower the bandgap of TiO<sub>2</sub> by adding new energy levels above VB and enable electron excitation from VB to CB. Nonmetal dopants such as N, C, S, and P are often applied to reduce the TiO<sub>2</sub> band gap and hence increase the absorption of visible light [22,78]. Nor & Amin [79] investigated glucose precursor C-doped TiO<sub>2</sub> for improving CO<sub>2</sub> photoreduction efficiency to produce CH<sub>3</sub>OH. The photocatalytic performance of C-doped TiO<sub>2</sub> was recorded highest with 6 wt% glucose loading (6C-TiO<sub>2</sub>), with a CH<sub>3</sub>OH yield of 19.5 mmol g<sup>-1</sup> h<sup>-1</sup>, which is 2-fold higher than pure TiO<sub>2</sub> at 9.5 mmol g<sup>-1</sup> h<sup>-1</sup>. The computed E<sub>CB</sub> for TiO<sub>2</sub> was 0.41 eV and for 6C-TiO<sub>2</sub> was 0.27 eV, respectively, while the E<sub>VB</sub> for TiO<sub>2</sub> and 6C-TiO<sub>2</sub> were 2.96 eV and 2.86 eV, respectively, indicating that the redox potential of the VB for both samples were sufficient to stimulate holes as electron acceptors. Bjelajac et al. [80] reported that doping of N nanoparticle to commercial P25 TiO<sub>2</sub> powder increased the CO<sub>2</sub> photoreduction activity. The average CH<sub>4</sub> production rate was found to be 0.191 μmol g<sup>-1</sup> h<sup>-1</sup>, while the CO production rate was μmol g<sup>-1</sup> h<sup>-1</sup>.

Substitutional nonmetal doping often presents defect states concentrated at the impurity location, lowering the band gap, and creating apparent absorption capacity [22]. As the degree of nonmetal doping increases, the defects rate also improves, and hence the photocatalytic activity hinders. As a result, considerable care must be taken in nonmetal doping to optimize the dopant concentration for higher visible light absorption and enhanced photocatalytic activity while maintaining an acceptable level of defects [22,81]. Co-doping using an electron donor-acceptor pair is a typical technique for reducing charge recombination in nonmetal doped TiO<sub>2</sub>. Recently, Foghani et al. [81] used Cu/P co-doped g-C<sub>3</sub>N<sub>4</sub>@TiO<sub>2</sub> photocatalyst for improving visible light photocatalytic CO<sub>2</sub> reduction. The results showed that P and Cu doping increased the specific surface area, reduced the band gap energy and recombination rate while extending light adsorption to the visible region. The optimum CH<sub>3</sub>OH production yield was recorded 859 μmol g<sup>-1</sup>

h<sup>-1</sup>, nearly 5 and 11.6 times greater than g-C<sub>3</sub>N<sub>4</sub> and TiO<sub>2</sub>, respectively.

### 3.4.4. Carbon based material doping

The synthesis of carbon-based materials with TiO<sub>2</sub> is an appealing approach in the field of photocatalytic activity. This is due to the availability, affordability, high specific surface area, substantial corrosion resistance, strong electrical and thermal conductivity, and controllable surface properties of carbon-based materials [82]. Most used carbon-based materials into TiO<sub>2</sub> catalysts are graphene, graphene oxide (GO), reduced graphene oxide (rGO), carbon nanotubes (CNTs), and carbon quantum dots (CQDs) for improving CO<sub>2</sub> photoreduction [83,84]. Wang et al. [20] examined porous hyper-crosslinked polymer-TiO<sub>2</sub>-graphene composite photocatalysts for CO<sub>2</sub> conversion under visible light irradiation. The constructed composite structure had a large surface area of 988 m<sup>2</sup> g<sup>-1</sup> and a high CO<sub>2</sub> uptake capability of 12.87 wt %. This composite exhibited excellent photocatalytic activity, particularly for CH<sub>4</sub> generation (27.62 μmol g<sup>-1</sup> h<sup>-1</sup>). Yang et al. [85] constructed TiO<sub>2</sub> spherical shells with modified by graphene to enhance photocatalytic activity for CO<sub>2</sub> reduction. This double-sided modification technique substantially enhanced the shell's contact area, allowing more photoelectrons to be separated from both sides of the shell. The main product was CO, with a little amount of CH<sub>4</sub> detected. Olowoyo et al. [86] synthesized reduced graphene oxide-TiO<sub>2</sub> composites for improving CO<sub>2</sub> photoreduction to CH<sub>3</sub>OH. They found that due to the alteration in the band gap and promoting the separation of photo-generated carriers photocatalytic CO<sub>2</sub> reduction was improved, providing a CH<sub>3</sub>OH generation rate of 2.33 mmol g<sup>-1</sup> h<sup>-1</sup>. Fernández-Catalá et al. [87] investigated Cu<sub>x</sub>O-doped TiO<sub>2</sub> photocatalyst adapted with CNTs for CO<sub>2</sub> photoreduction. Using low-power LED lighting, they identified a CH<sub>4</sub> generation rate of 117 μmol g<sup>-1</sup> h<sup>-1</sup>, which was the highest values documented for any reactor design or catalytic system. The choice of an appropriate hole scavenger and successive tuning of its concentration were crucial in achieving such CH<sub>4</sub> production rates.

Some studies have shown that when TiO<sub>2</sub> nanostructured materials, particularly TiO<sub>2</sub> nanotubes (TNTs) and TiO<sub>2</sub> nanorods (TNRs), are

treated with reduced graphene oxide and carbon quantum dots, photocatalytic CO<sub>2</sub> conversion activity is significantly increased. For instance, Khatun et al. [88] prepared rGO modified TNTs as visible light supportive catalyst for reducing CO<sub>2</sub> to CH<sub>4</sub>. TNTs with rGO inserted showed a higher rate of electron-hole separation. The increased photocatalytic activity of rGO with TNTs was confirmed by increased CO<sub>2</sub> to CH<sub>4</sub> conversion, which resulted in improved CH<sub>4</sub> generation (9.27%), which is 1.81-fold greater than the CH<sub>4</sub> generation rate obtained with TNTs (5.12%). In another study, modification of TNTs with biomass derived CQDs for enhanced CO<sub>2</sub> photoreduction was carried out by Zhang et al. [89]. The CO<sub>2</sub> photoreduction is found highest in the composite generated by combining 10 mL of CQDs solution with TNTs, yielding CO and CH<sub>4</sub> of 13.55 and 3.54 μmol g<sup>-1</sup> h<sup>-1</sup>, respectively, which are 2.4 and 2.5-fold that of TNTs. Liu et al. [90] synthesized rod-like TiO<sub>2</sub> modified rGO composite for highly efficient visible-light driven CO<sub>2</sub> photoreduction. The produced composite had a large specific surface area of 287.3 m<sup>2</sup>/g with pore volume of 0.72 cm<sup>3</sup>/g, allowing for excellent reactant absorption and rapid intraparticle molecular transfer. CO<sub>2</sub> was successfully converted to methanol (MeOH), methane (CH<sub>4</sub>), ethanol (EtOH), and dimethyl ether (DME) using the composite (Fig. 14a). The total carbon yield of G-25Ti (TiO<sub>2</sub>-rGO with 25 mmol Ti<sup>4+</sup>) was found to be 15.7 times greater than that of pristine P25 (Fig. 14b). Carbon conversion was shown to be more than 6 times higher in P25 doped rGO composites than in pure P25. The order of CO<sub>2</sub> conversion, according to their findings, is G-25Ti > G-20Ti > G-15Ti, depending on the amount of rGO present.

### 3.4.5. Dispersion on supports

The dispersion of TiO<sub>2</sub> on different types of supports improves the electronic properties, product selectivity as well as pore structure of catalysts [22]. Besides, this modification strategy also overcomes the requirement for post-treatment dissociation and offers a large surface area. This approach has two key challenges: low mass transfer rate and light absorption efficacy. TiO<sub>2</sub> photocatalysts can be immobilized on substrates like fibers, membranes, glass, carbonaceous materials, silica, and clays through dip or spin coating [91]. Dip coating is usually recommended over spin coating because of its scale-up adaptability, improved controllability, superior structural and optical properties [22].

Tasbihi et al. [92] examined the photocatalytic performance of mesoporous silica-supported dip-coated Pt/TiO<sub>2</sub> for CO<sub>2</sub> photoreduction to CH<sub>4</sub>. All photocatalysts had substantial carbon products of CH<sub>4</sub> and CO, with low quantities of CH<sub>3</sub>OH. It has been discovered that supporting Pt/TiO<sub>2</sub> catalysts on mesoporous silica protects the reaction's selectivity for CH<sub>4</sub> production and increases the activity of Pt/TiO<sub>2</sub> photocatalysts. For CO<sub>2</sub> photoreduction to produce CH<sub>4</sub>, Larimi et al. [93] evaluated the photocatalytic performance of carbonaceous materials supported photocatalysts coated with Pt-TiO<sub>2</sub>. Photocatalytic performances of the synthesized photocatalysts were influenced by the particle size and carbonaceous supports applied and followed an order: multi-walled CNTs > single-walled CNTs > rGO > activated carbon. When compared to other samples, Pt-TiO<sub>2</sub>/multi-walled carbon nanotubes had greater catalytic activity and reached a maximum yield of CH<sub>4</sub> (1.9 μmol g<sup>-1</sup> h<sup>-1</sup>). The photocatalytic activity of glass supported NiO/TiO<sub>2</sub> photocatalysts was explored by Ku et al. [94] for photoreduction of gaseous CO<sub>2</sub> to hydrocarbon fuels. They observed that the distribution of Ni, Ti, and O atoms on the surface of these photocatalysts was consistent, and that the BET surface areas varied slightly as NiO loading increased. Meanwhile, the absorption edge of produced photocatalysts has shifted towards the visible region, lowering the bandgap energy. Methane was identified to be the main product and maximum production (4.69 mmol g<sup>-1</sup> h<sup>-1</sup>) was recorded for 10 wt% NiO/TiO<sub>2</sub> loading which was 2-fold higher than pure TiO<sub>2</sub>.

### 3.4.6. Surface sensitization

Surface sensitization is vital for increasing the efficiency of photoexcitation processes and expanding the photocatalyst's useable light

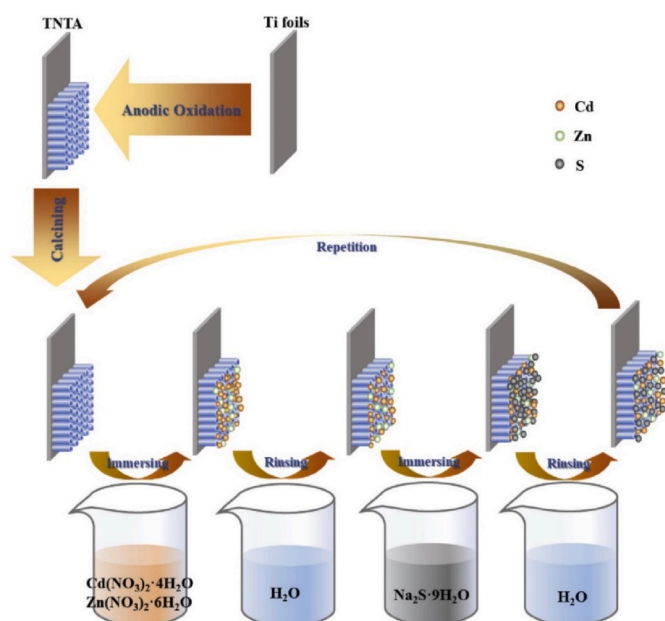


Fig. 15. Experimental illustration of surface sensitization with CdS/ZnS on TiO<sub>2</sub> nanotube arrays (Adopted from Ref. [97] with permission from Elsevier).

wavelength through excitation [78]. The sensitizers can improve the visible light utilization of a semiconductor photocatalysts [95]. The semiconductor is mostly used as a charge carrier instead of a generator of electrons and holes, and the process is extremely fast. Sensitizers based on dyes are one of the most extensively used sensitizers. The dye and semiconductor (TiO<sub>2</sub>) have different roles in dye sensitization process, with TiO<sub>2</sub> acting as an electron acceptor and the dye acting as a light harvester. Jo et al. [96] synthesized light-sensitized squaraine (SQ) dyes and merged them into dye-sensitized catalysts (DSCs) with combination of SQ/TiO<sub>2</sub>/Cat, and their efficacies were assessed in terms of CO<sub>2</sub> reduction rate. After the induction time, the photodegraded SQ was found to function as a true photosensitizer under high energy irradiation (>400 nm), yielding 16.5 μmol for 70 h.

Under visible light irradiation, Cheng et al. [97] evaluated the photocatalytic conversion performance of gas phase CO<sub>2</sub> by TNT arrays sensitized with CdS/ZnS quantum dots. The method of successive ionic layer adsorption (SILAR) was used to deposit CdS/ZnS composite as quantum dots (QDs) onto TNTA, as shown in Fig. 15. As the SILAR cycle number increased, the yield of principal product (methanol) enhanced and then reduced, and the performance of CdS/ZnS-TNTA was recorded 2.73 times higher than pristine TNTA. Chon et al. [98] developed an InP-QD-sensitized hybrid photocatalyst (InP-QD/TiO<sub>2</sub>/ReP) and tested it as a low-energy photosensitizer. It was observed that the photoexcited electron transfer mechanism from the photoexcited InP-QD\* to the inorganic TiO<sub>2</sub> solid is aided by InP quantum dot sensitization on the TiO<sub>2</sub> surface, leading to higher charge separation at the InP-QD/TiO<sub>2</sub> interface. The InP-QD-sensitized TiO<sub>2</sub> hybrid (InP-QD/TiO<sub>2</sub>/ReP) displayed highly efficient and reliable photocatalytic CO<sub>2</sub>-to-CO conversion activity in a single run under comparatively lower energy irradiation (>500 nm), with a turnover number of 2500 for 26 h.

### 3.4.7. Heterojunction

Heterostructures synthesis is undoubtedly the most effective approach presently being used for improving the photocatalytic performance of TiO<sub>2</sub> [78]. Heterostructure is developed by integrating two semiconductors that have compatible characteristics that allow the heterostructure to show better performance than the individual semiconductors [99]. The photoreaction in a heterostructure commences with photocatalytic reaction and excitation of the individual semiconductor materials that make up the heterostructure, just as it does in

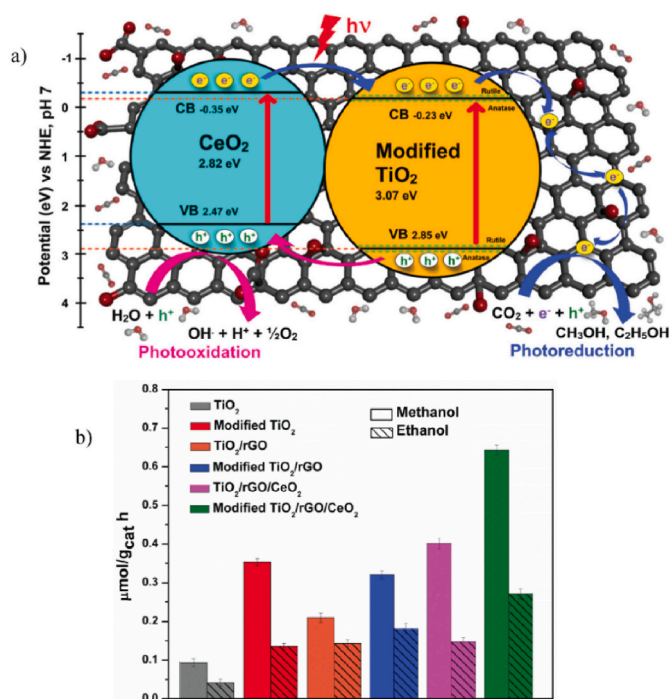


**Fig. 16.** Heterojunction photocatalysts for CO<sub>2</sub> photoreduction (a) photoreduction mechanism of modified TiO<sub>2</sub>/rGO/CeO<sub>2</sub> photocatalysts and (b) CH<sub>3</sub>OH and C<sub>2</sub>H<sub>5</sub>OH yields for various photocatalysts (Adopted from Ref. [100] with permission from Elsevier).

all pure photocatalysts. Seeharaj et al. [100] developed heterojunction photocatalysts by mixing surface modified titanium dioxide (TiO<sub>2</sub>) nanoparticles with rGO and cerium oxide (CeO<sub>2</sub>) for conversion of CO<sub>2</sub> to CH<sub>3</sub>OH and C<sub>2</sub>H<sub>5</sub>OH. The mechanism of CO<sub>2</sub> photoreduction to produce CH<sub>3</sub>OH and C<sub>2</sub>H<sub>5</sub>OH by utilizing TiO<sub>2</sub>/rGO/CeO<sub>2</sub> composite

photocatalysts is depicted in Fig. 16a. The customized TiO<sub>2</sub>/rGO/CeO<sub>2</sub> photocatalysts showed excellent photocatalytic activity by generating CH<sub>3</sub>OH at 641 μmol g<sup>-1</sup> h<sup>-1</sup> and C<sub>2</sub>H<sub>5</sub>OH at 271 μmol g<sup>-1</sup> h<sup>-1</sup>, almost 7-fold higher than pristine TiO<sub>2</sub> (Fig. 16b).

TiO<sub>2</sub>-based heterojunction can be classified into three types for photoreduction of CO<sub>2</sub> considering the charge carrier separation process: typical type II, direct Z-scheme, and S-scheme heterojunction [101, 102]. Table 3 presents the summary of recent studies conducted using these types of heterojunction methods for photocatalytic CO<sub>2</sub> photoreduction. The most common heterojunction approach for improving TiO<sub>2</sub>'s CO<sub>2</sub> reduction efficiency is type-II heterojunction. Coupling semiconductor type-A with a higher CB and semiconductor type-B with a lower VB can generate a standard type-II heterojunction photocatalyst. Wang et al. [103] found the greatest production of CH<sub>4</sub> among the research on type II heterojunction shown in Table 3. They evaluated the photocatalytic performance of produced g-C<sub>3</sub>N<sub>4</sub>/TiO<sub>2</sub> photocatalysts after exposing them to an 8W UV lamp for 4 h. Z-scheme type of heterojunction is comprised of two semiconductors connected by appropriate intermediate couples. The Z-scheme heterojunction is increasingly employed because to its high electron-hole separation rate, robust redox ability, and wide range of light response [104]. Recently, Kamal et al. [105] developed plasmonic Au nanoparticles that were photo-deposited on a TiO<sub>2</sub>-coated N-doped graphene heterostructure catalyst, resulting in significantly increased CO<sub>2</sub> reduction activity and good selectivity for methane generation. Researchers are moving forward with the Step-scheme (S-scheme) heterojunction approach due to some drawbacks of the two methods previously described. S-scheme heterojunction is made up of staggered band reduction and oxidation photocatalysts, and it's comparable to a type-II heterojunction just with an entirely distinct charge-transfer mechanism [106]. Tahir & Tahir [107] synthesized a ternary g-C<sub>3</sub>N<sub>4</sub>/TiO<sub>2</sub>/Ti<sub>3</sub>AlC<sub>2</sub> S-scheme heterojunction photocatalyst to obtain the highest CH<sub>4</sub> yield of 2103.5 μmol g<sup>-1</sup> h<sup>-1</sup> with 96.59% selectivity.

**Table 3**

Summary of recent photocatalytic CO<sub>2</sub> reductions using various types of heterojunction modification methods.

Photocatalyst	Reductant	Reactor	Mode of heterojunction	Type of light	Product	Yield (μmol g <sup>-1</sup> h <sup>-1</sup> )	References	
BiVO <sub>4</sub> /Bi <sub>4</sub> Ti <sub>3</sub> O <sub>12</sub>	CO <sub>2</sub> +H <sub>2</sub> O vapor	Schlenk flask reactor	Type II	300W Xe lamp	CH <sub>3</sub> OH	16.61	[108]	
g-C <sub>3</sub> N <sub>4</sub> /TiO <sub>2</sub>	Triethanolamine + NaOH	Photochemical reactor		8W UV lamp	CO CH <sub>4</sub>	13.29 72.2	[103]	
In <sub>2</sub> S <sub>3</sub> /TiO <sub>2</sub>	CO <sub>2</sub> + H <sub>2</sub> O	Stainless steel reactor	Z-scheme	300W Xe lamp	CO	56.2	[109]	
Pt-SrTiO <sub>3</sub>	CO <sub>2</sub> +H <sub>2</sub> O	Gas-closed circulation system		300W	CH <sub>4</sub>	26.7		[110]
SnS <sub>2</sub> -Ti <sup>3+</sup> /TiO <sub>2</sub>	Dimethylformamide + H <sub>2</sub> O	Pyrex reactor		Xe lamp Simulated solar light	CO	58	[111]	
ZnFe <sub>2</sub> O <sub>4</sub> /Ag/TiO <sub>2</sub>	CO <sub>2</sub> +H <sub>2</sub> O	Fixed bed photoreactor		200W Hg lamp	CO	1025	[112]	
CuCo <sub>2</sub> S <sub>4</sub> @3B-TiO <sub>2</sub>	CO <sub>2</sub> +H <sub>2</sub> O	Batch liquid-gas photoreactor		250W Hg lamp	CH <sub>4</sub> CH <sub>3</sub> OH CH <sub>4</sub>	132 30.8 42.2	[113]	
Au-NG-TiO <sub>2</sub>	CO <sub>2</sub> + NaHCO <sub>3</sub>	Quartz reactor	S-scheme	300W Xe lamp	CO	25.5	[105]	
CdS/TiO <sub>2</sub>	CO <sub>2</sub> +H <sub>2</sub> O	Quartz reactor		350 W Xe lamp	CH <sub>4</sub>	742.4 27.85		[114]
TiO <sub>2</sub> /polydopamine	CO <sub>2</sub> +H <sub>2</sub> O	Pyrex glass reactor		350 W Xe lamp	CH <sub>4</sub>	1.5		[21]
CsPbBr <sub>3</sub> @ mesoporous TiO <sub>2</sub>	CO <sub>2</sub> +H <sub>2</sub> O+ C <sub>4</sub> H <sub>8</sub> O <sub>2</sub>	Sealed circulation reactor		300 W Xe lamp	CH <sub>3</sub> OH CH <sub>4</sub>	0.26 145.28	[115]	
g-C <sub>3</sub> N <sub>4</sub> /TiO <sub>2</sub> /Ti <sub>3</sub> AlC <sub>2</sub>	CO <sub>2</sub> +H <sub>2</sub> O	Fixed bed monolith photoreactor		35 W HID car lamp	CH <sub>4</sub>	2103.5	[107]	



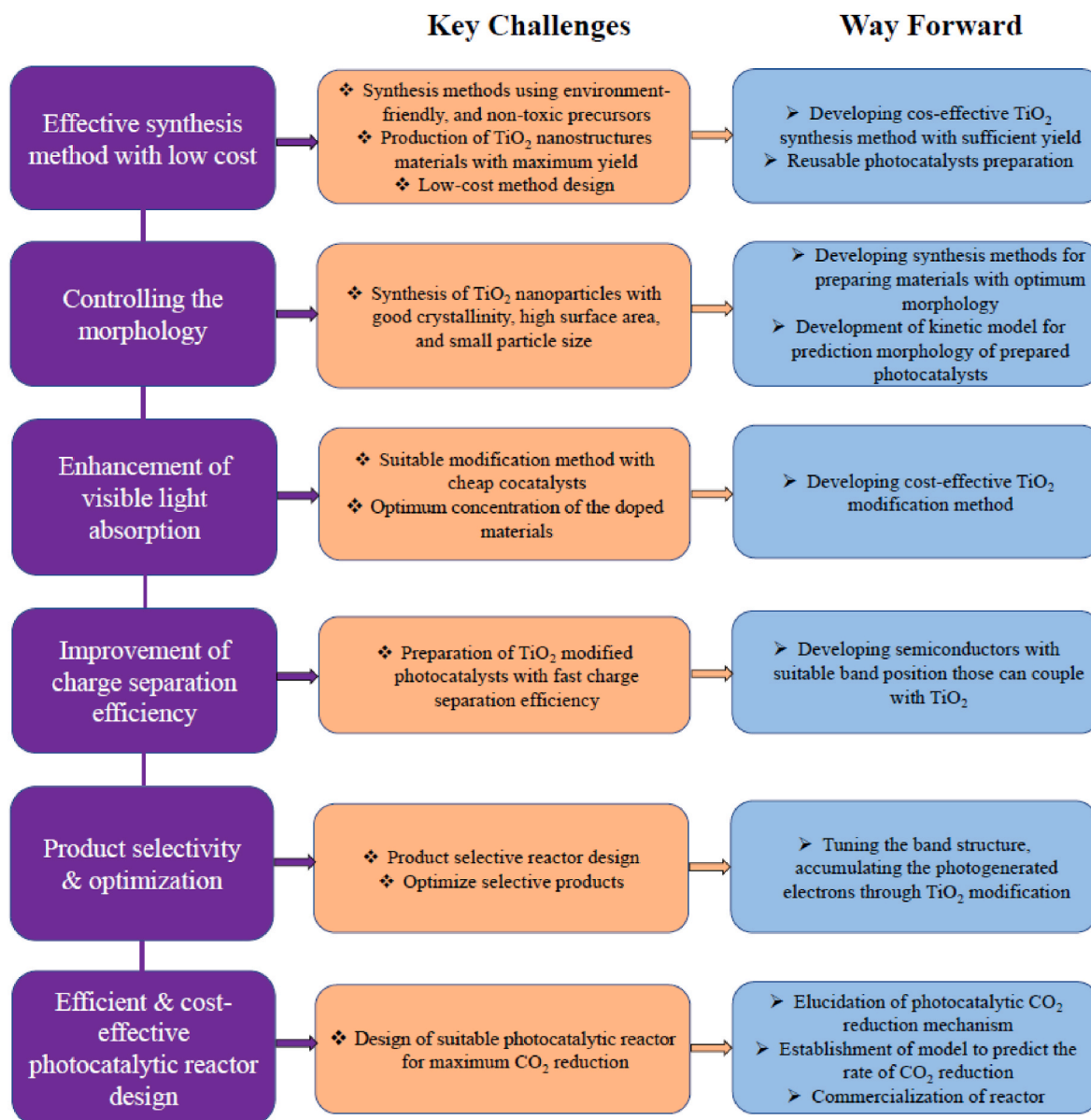


Fig. 17. Key challenges for CO<sub>2</sub> photoreduction to hydrocarbon fuels of TiO<sub>2</sub>-based photocatalysts.

### 3.5. Challenges for photocatalytic CO<sub>2</sub> reduction to hydrocarbon fuels

Enormous research works are ongoing to improve the performance of TiO<sub>2</sub>-based photocatalysts for CO<sub>2</sub> photoreduction. However, there are still a lot of challenges to be solved for practical application of TiO<sub>2</sub> as a photocatalyst to efficiently use sunlight and CO<sub>2</sub> for the production of hydrocarbon fuels. These are presented in Fig. 17 along with suggestions to address them and are discussed in more detail below.

- Synthesis methods are very crucial that directly influence the properties of photocatalysts as well as whole photocatalytic process. Developing cost effective synthesis method with sufficient yield of photocatalyst is a big challenge. Future research should concentrate on developing novel synthesis techniques using affordable, environmentally friendly, and non-toxic precursors for the production of reusable photocatalyst materials.
- Synthesis of TiO<sub>2</sub> nanostructures materials with a desired morphology such as pore size, length, and wall thickness have great influence on photocatalytic CO<sub>2</sub> reduction efficiency. Electrochemical anodization is a promising approach in the preparation of

TiO<sub>2</sub> nanoparticles since this method has the scope to tune materials with required morphology and quantity by adjusting different anodization parameters. There is a scope to work on the development of kinetic model to predict the morphology of prepared photocatalyst.

- The initial phase in photocatalysis is the absorption of light; more light absorption leads to increased electron-hole formation on the photocatalytic surface, which enhances photocatalytic CO<sub>2</sub> reduction. Thus, the enhancement of this process under visible light is a critical step in hydrocarbon fuels production activity. Generally different modification methods are used for improving the performance of photocatalysts under visible light irradiation. Finding the optimal percentage of the doped materials is the key issue in the surface modification process. For its broad range of practical applications, the recyclability modified photocatalysts is also vital. Even a photocatalyst with excellent photoconversion potential, will not be treated as feasible if its long-term stability is insufficient. Therefore, for practical application of TiO<sub>2</sub> in CO<sub>2</sub> photoreduction, it is indispensable to develop a suitable photocatalyst in terms of stability and efficiency through surface modification.



- The performance of TiO<sub>2</sub> photocatalysts for CO<sub>2</sub> photoreduction also depends on the charge separation process. After the excitation phase, the electron-hole must be successfully separated and moved to the photocatalyst's surface to start the redox reaction. The charge carriers will recombine if this process is not carried out as quickly as possible. Noble metals were used as a co-catalyst in the majority of published research to increase charge separation efficiency, however these metals are quite expensive. Therefore, research should be done to find appropriate cheaper and available transition metals. Additionally, composite construction between two semiconductors with appropriate band positions may also be able to enhance the performance of charge separation. However, since not all semiconductors can couple with TiO<sub>2</sub>, finding semiconductors that fulfil the specifications may be challenging.
- It is usually recognized that photocatalytic CO<sub>2</sub> reduction can produce a variety of products. To optimize targeted product and for understanding CO<sub>2</sub> photoreduction mechanism, product selectivity has great importance. To make the subsequent separation step easier, a good selectivity of particular hydrocarbon fuel production is greatly preferred. The end product of photocatalytic CO<sub>2</sub> reduction is strongly influenced by both the redox potential and surface density of electron. Thus, a potential way to manage the photocatalytic CO<sub>2</sub> reduction's selectivity is by modifying the TiO<sub>2</sub> band structure. Furthermore, it is also vital to establish a rigorous, reliable, and stable system for product detection.
- Finally, away from the synthesis and modification of photocatalyst material, photocatalytic reactor design and understanding the reaction mechanism are other major areas for CO<sub>2</sub> photoreduction to hydrocarbon fuels. The yield of CO<sub>2</sub> photoreduction depends mainly on intensity of incident light and photocatalysis material and photoreactor used. However, proper photoreactor design and a deeper understanding of the reaction mechanism in photoreactor are the only ways to significantly increase the performance of photocatalytic materials. The studies of CO<sub>2</sub> photoreduction to date have mainly focused on the overall yield of the products. For further utilization of TiO<sub>2</sub> modification, detailed research on the CO<sub>2</sub> photoreduction mechanism on the TiO<sub>2</sub> surface is still lacking. On a broad scale, there is still little understanding of reaction mechanisms, reaction routes, and kinetic and thermodynamic studies of the CO<sub>2</sub> photoreduction process. The use of photocatalytic materials will be improved by more study in the fields of photochemistry and surface chemistry, which will result in a deeper understanding of the activities occurring at the photocatalyst's surface. This kind of strategy will provide a comprehensive and sustainable evaluation of photocatalytic CO<sub>2</sub> reduction to hydrocarbon fuels and its potential as a long-term strategy to address greenhouse gas emissions and energy production.

#### 4. Conclusion

This systematic review was conducted in respect to address the recent advances in CO<sub>2</sub> photoreduction along with future challenges to produce hydrocarbon fuels. From 17 countries of the world 62 articles were identified for review based on the selection criteria. Recent advancements in TiO<sub>2</sub>-based photocatalysts and the development of modification strategies for photocatalytic CO<sub>2</sub> reduction have been systematically examined in this review. More importantly, this review highlighted the influencing factors affect photocatalytic CO<sub>2</sub> reduction performance over TiO<sub>2</sub>-based photocatalysts. However, despite of intensive research on this dream prospective area, the production rates of hydrocarbon fuels rarely exceed  $\mu\text{mol g}^{-1} \text{h}^{-1}$ . Even though, significant improvements have been made in terms of theoretical development, surface modification and performance of TiO<sub>2</sub>-based CO<sub>2</sub> photoreduction approach, it is still long way to go for practical applications. Researchers can utilize this review to set their future goals and efforts in establishing novel methodologies while taking the challenges

into consideration.

#### Declaration of competing interest

The authors declare that they have no known competing financial interests or personal relationships that could have appeared to influence the work reported in this paper.

#### Data availability

The authors are unable or have chosen not to specify which data has been used.

#### Acknowledgement

This study was supported by the Universiti Malaysia Pahang (UMP) Postgraduate Research Scheme (PGRS220347). The authors express gratitude for the grant.

#### References

- [1] N. Shen, Y. Wang, H. Peng, Z. Hou, Renewable energy green innovation, fossil energy consumption, and air pollution-spatial empirical analysis based on China, *Sustain. Times* 12 (16) (2020) 1–23, <https://doi.org/10.3390/SU12166397>.
- [2] A. Rehman, H. Ma, I. Ozturk, Do industrialization, energy importations, and economic progress influence carbon emission in Pakistan, *Environ. Sci. Pollut. Res.* 28 (33) (2021) 45840–45852, <https://doi.org/10.1007/s11356-021-13916-4>.
- [3] J.L. Ramos, B. Pakuts, P. Godoy, A. García-Franco, E. Duque, Addressing the energy crisis: using microbes to make biofuels, *Microb. Biotechnol.* 15 (4) (2022) 1026–1030, <https://doi.org/10.1111/1751-7915.14050>.
- [4] S. Nalley, A. Larose, IEO2021 Highlights, vol. 2021, *Energy Inf. Adm.*, 2021, p. 21 [Online]. Available: [https://www.eia.gov/outlooks/ieo/pdf/IEO2021\\_ReleasePresentation.pdf](https://www.eia.gov/outlooks/ieo/pdf/IEO2021_ReleasePresentation.pdf).
- [5] A. Friedemann, *Life after Fossil Fuels: A Reality Check on Alternative Energy*, Springer International Publishing, London, UK, 2021.
- [6] J.L. Holeczek, H.M.E. Geli, M.N. Sawalrah, R. Valdez, A. Global Assessment, Can renewable energy replace fossil fuels by 2050? *Sustain. Times* 14 (8) (2022) 1–22, <https://doi.org/10.3390/su14084792>.
- [7] N. Shehzad, M. Tahir, K. Johari, T. Murugesan, M. Hussain, A critical review on TiO<sub>2</sub> based photocatalytic CO<sub>2</sub> reduction system: strategies to improve efficiency, *J. CO<sub>2</sub> Util.* 26 (2018) 98–122, <https://doi.org/10.1016/j.jcou.2018.04.026>. November 2017.
- [8] K. Perera F, Nadeau, Climate change, fossil-fuel pollution, and children's health, *N. Engl. J. Med.* 386 (24) (2022) 2303–2314, <https://doi.org/10.1056/NEJMr2117706>.
- [9] US EPA, Global Greenhouse Gas Emissions Data, 2020 [Online]. Available: <https://www.epa.gov/ghgemissions/global-greenhouse-gas-emissions-data>.
- [10] IEA, British Petroleum Statistical Review of World Energy, 2022 [Online]. Available: <https://www.bp.com/content/dam/bp/businesssites/en/global/corporate/pdfs/energy-economics/statistical-review/bp-stats-review-2022-full-report.pdf>.
- [11] E. Gong, et al., Solar fuels: research and development strategies to accelerate photocatalytic CO<sub>2</sub> conversion into hydrocarbon fuels, *Energy Environ. Sci.* 15 (3) (2022) 880–937, <https://doi.org/10.1039/d1ee02714j>.
- [12] J. Wu, J. Liu, W. Xia, Y.Y. Ren, F. Wang, Advances on photocatalytic CO<sub>2</sub> reduction based on CdS and CdSe nano-semiconductors, *Wuli Huaxue Xuebao/Acta Phys. - Chim. Sin.* 37 (5) (2021) 1–8, <https://doi.org/10.3866/PKU.WHXB202008043>.
- [13] Z. Wang, et al., Recent progress of perovskite oxide in emerging photocatalysis landscape: water splitting, CO<sub>2</sub> reduction, and N<sub>2</sub> fixation, *Wuli Huaxue Xuebao/Acta Phys. - Chim. Sin.* 37 (6) (2021) 1–31, <https://doi.org/10.3866/PKU.WHXB202011033>.
- [14] Z. Qin, J. Wu, B. Li, T. Su, H. Ji, Ultrathin layered catalyst for photocatalytic reduction of CO<sub>2</sub>, *Wuli Huaxue Xuebao/Acta Phys. - Chim. Sin.* 37 (5) (2021) 1–21, <https://doi.org/10.3866/PKU.WHXB202005027>.
- [15] I. Ibrahim, et al., Silver decorated TiO<sub>2</sub>/g-C<sub>3</sub>N<sub>4</sub> bifunctional nanocomposites for photocatalytic elimination of water pollutants under UV and artificial solar light, *Results Eng* 14 (April) (2022), 100470, <https://doi.org/10.1016/j.rineng.2022.100470>.
- [16] T.P. Nguyen, et al., Recent advances in TiO<sub>2</sub>-based photocatalysts for reduction of CO<sub>2</sub> to fuels, *Nanomaterials* 10 (2) (2020) 1–24, <https://doi.org/10.3390/nano10020337>.
- [17] A. Shoneye, J. Sen Chang, M.N. Chong, J. Tang, Recent progress in photocatalytic degradation of chlorinated phenols and reduction of heavy metal ions in water by TiO<sub>2</sub>-based catalysts, *Int. Mater. Rev.* 67 (1) (2022) 47–64, <https://doi.org/10.1080/09506608.2021.1891368>.
- [18] M. Zu, et al., Sustainable engineering of TiO<sub>2</sub>-based advanced oxidation technologies: from photocatalyst to application devices, *J. Mater. Sci. Technol.* 78 (2021) 202–222, <https://doi.org/10.1016/j.jmst.2020.10.061>.

- [19] O. Shtyka, et al., Adsorption and photocatalytic reduction of carbon dioxide on TiO<sub>2</sub>, *Catalysts* 11 (1) (2021) 1–12, <https://doi.org/10.3390/catal11010047>.
- [20] S. Wang, et al., Porous hypercrosslinked polymer-TiO<sub>2</sub>-graphene composite photocatalysts for visible-light-driven CO<sub>2</sub> conversion, *Nat. Commun.* 10 (1) (2019), <https://doi.org/10.1038/s41467-019-08651-x>.
- [21] A. Meng, B. Cheng, H. Tan, J. Fan, C. Su, J. Yu, TiO<sub>2</sub>/polydopamine S-scheme heterojunction photocatalyst with enhanced CO<sub>2</sub>-reduction selectivity, *Appl. Catal. B Environ.* 289 (2021) 120039, <https://doi.org/10.1016/j.apcatb.2021.120039>, February.
- [22] S. Al Jitan, G. Palmisano, C. Garlisi, Synthesis and surface modification of TiO<sub>2</sub>-based photocatalysts for the conversion of CO<sub>2</sub>, *Catalysts* 10 (2) (2020), <https://doi.org/10.3390/catal10020227>.
- [23] C.B. Anucha, I. Altin, E. Bacaksiz, V.N. Stathopoulos, Titanium dioxide (TiO<sub>2</sub>)-based photocatalyst materials activity enhancement for contaminants of emerging concern (CECs) degradation: in the light of modification strategies, *Chem. Eng. J. Adv.* 10 (2022) 100262, <https://doi.org/10.1016/j.cej.2022.100262>, February.
- [24] S. Kreft, D. Wei, H. Junge, M. Beller, Recent advances on TiO<sub>2</sub>-based photocatalytic CO<sub>2</sub> reduction, *Energy* 2 (6) (2020), <https://doi.org/10.1016/j.enchem.2020.100044>.
- [25] Z. Bahadoran, P. Mirmiran, K. Kashfi, A. Ghasemi, Importance of systematic reviews and meta-analyses of animal studies: challenges for animal-to-human translation, *J. Am. Assoc. Lab. Anim. Sci.* 59 (5) (2020) 469–477, <https://doi.org/10.30802/AALAS-JAALAS-19-000139>.
- [26] H.A. Mohamed Shaffril, A.A. Samah, S.F. Samsuddin, Z. Ali, Mirror-mirror on the wall, what climate change adaptation strategies are practiced by the Asian's fishermen of all? *J. Clean. Prod.* 232 (2019) 104–117, <https://doi.org/10.1016/j.jclepro.2019.05.262>.
- [27] S. Echchakoui, Why and how to merge Scopus and Web of Science during bibliometric analysis: the case of sales force literature from 1912 to 2019, *J. Mark. Anal.* 8 (3) (2020) 165–184, <https://doi.org/10.1057/s41270-020-00081-9>.
- [28] N.T. Sahrin, R. Nawaz, F.K. Chong, S.L. Lee, M.D.H. Wirzal, Current perspectives of anodized TiO<sub>2</sub> nanotubes towards photodegradation of formaldehyde: a short review, *Environ. Technol. Innovat.* 22 (2021), 101418, <https://doi.org/10.1016/j.eti.2021.101418>.
- [29] S.Z. Ran, J. M. Jaroniec, Qiao, Advanced materials - 2018 - ran - cocatalysts in semiconductor-based photocatalytic CO<sub>2</sub> reduction achievements challenges, *Adv. Mater.* 30 (2018), <https://doi.org/10.1002/adma.201704649>, 1704649.
- [30] C. Byrne, G. Subramanian, S.C. Pillai, Recent advances in photocatalysis for environmental applications, *J. Environ. Chem. Eng.* 6 (3) (2018) 3531–3555, <https://doi.org/10.1016/j.jece.2017.07.080>.
- [31] M. Ismael, A review on graphitic carbon nitride (g-C<sub>3</sub>N<sub>4</sub>) based nanocomposites: synthesis, categories, and their application in photocatalysis, *J. Alloys Compd.* 846 (2020), 156446, <https://doi.org/10.1016/j.jallcom.2020.156446>.
- [32] H.L. Tan, F.F. Abdi, Y.H. Ng, Heterogeneous photocatalysts: an overview of classic and modern approaches for optical, electronic, and charge dynamics evaluation, *Chem. Soc. Rev.* 48 (5) (2019) 1255–1271, <https://doi.org/10.1039/c8cs00882e>.
- [33] J. Yan, et al., Photothermal synergic enhancement of direct Z-scheme behavior of Bi<sub>4</sub>TaO<sub>9</sub>Cl/W<sub>18</sub>O<sub>49</sub> heterostructure for CO<sub>2</sub> reduction, *Appl. Catal. B Environ.* 268 (October 2019) 2020, <https://doi.org/10.1016/j.apcatb.2019.118401>.
- [34] H. Ma, C. Wang, S. Li, X. Zhang, Y. Liu, High-humidity tolerance of porous TiO<sub>2</sub>(B) microspheres in photothermal catalytic removal of NO<sub>x</sub>, *Chin. J. Catal.* 41 (10) (2020) 1622–1632, [https://doi.org/10.1016/S1872-2067\(19\)63508-4](https://doi.org/10.1016/S1872-2067(19)63508-4).
- [35] D. Li, et al., Thermal coupled photoconductivity as a tool to understand the photothermal catalytic reduction of CO<sub>2</sub>, *Chin. J. Catal.* 41 (1) (2020) 154–160, [https://doi.org/10.1016/S1872-2067\(19\)63475-3](https://doi.org/10.1016/S1872-2067(19)63475-3).
- [36] F. Yu, et al., Enhanced solar photochemical catalysis over solution plasma activated TiO<sub>2</sub>, *Adv. Sci.* 7 (2020) 16, <https://doi.org/10.1002/advs.202000204>.
- [37] P.R. Yaashikaa, P. Senthil Kumar, S.J. Varjani, A. Saravanan, A review on photochemical, biochemical and electrochemical transformation of CO<sub>2</sub> into value-added products, *J. CO<sub>2</sub> Util.* 33 (May) (2019) 131–147, <https://doi.org/10.1016/j.jcou.2019.05.017>.
- [38] M. Rosales, T. Zoltan, C. Yadarola, E. Mosquera, F. Gracia, A. García, The influence of the morphology of 1D TiO<sub>2</sub> nanostructures on photogeneration of reactive oxygen species and enhanced photocatalytic activity, *J. Mol. Liq.* 281 (2019) 59–69, <https://doi.org/10.1016/j.molliq.2019.02.070>.
- [39] A.B. Tesler, M. Altomare, P. Schmuki, Morphology and optical properties of highly ordered TiO<sub>2</sub> nanotubes grown in NH<sub>4</sub>F/o-H<sub>3</sub>PO<sub>4</sub> electrolytes in view of light-harvesting and catalytic applications, *ACS Appl. Nano Mater.* 3 (11) (2020) 10646–10658, <https://doi.org/10.1021/acsnm.0c01859>.
- [40] X. Li, J. Yu, and C. Jiang, Principle and Surface Science of Photocatalysis, vol. vol. 31. 2020.
- [41] D. Li, et al., Effects of particle size on the structure and photocatalytic performance by alkali-treated TiO<sub>2</sub>, *Nanomaterials* 10 (3) (2020) 1–14, <https://doi.org/10.3390/nano10030546>.
- [42] C. ying Huang, et al., One-dimension TiO<sub>2</sub> nanostructures with enhanced activity for CO<sub>2</sub> photocatalytic reduction, *Appl. Surf. Sci.* 464 (2019) 534–543, <https://doi.org/10.1016/j.apsusc.2018.09.114>, June 2018.
- [43] M. Kowalkińska, S. Dudziak, J. Karczewski, J. Ryl, G. Trykowski, A. Zielińska-Jurek, Facet effect of TiO<sub>2</sub> nanostructures from TiOF<sub>2</sub> and their photocatalytic activity, *Chem. Eng. J.* 404 (May 2020) 2021, <https://doi.org/10.1016/j.cej.2020.126493>.
- [44] N.T. Nguyen, et al., Providing significantly enhanced photocatalytic H<sub>2</sub> generation using porous PtPdAg alloy nanoparticles on spaced TiO<sub>2</sub> nanotubes, *Int. J. Hydrogen Energy* 44 (41) (2019) 22962–22971, <https://doi.org/10.1016/j.ijhydene.2019.06.200>.
- [45] L. Warmuth, et al., Catalytic CO oxidation and H<sub>2</sub>O<sub>2</sub> direct synthesis over pd and pt-impregnated titania nanotubes, *Catalysts* 11 (8) (2021) 1–11, <https://doi.org/10.3390/catal11080949>.
- [46] A. Das, P.M. Kumar, M. Bhagavathiachari, R.G. Nair, Hierarchical ZnO-TiO<sub>2</sub> nanoheterojunction: a strategy driven approach to boost the photocatalytic performance through the synergy of improved surface area and interfacial charge transport, *Appl. Surf. Sci.* 534 (2020), 147321, <https://doi.org/10.1016/j.apsusc.2020.147321>, June.
- [47] L. Wang, B. Cheng, L. Zhang, J. Yu, In situ irradiated XPS investigation on S-scheme TiO<sub>2</sub>@ZnIn<sub>2</sub>S<sub>4</sub> photocatalyst for efficient photocatalytic CO<sub>2</sub> reduction, *Small* 17 (41) (2021) 1–9, <https://doi.org/10.1002/sml.202103447>.
- [48] M.C. Wu, K.C. Hsiao, Y.H. Chang, S.H. Chan, Photocatalytic hydrogen evolution of palladium nanoparticles decorated black TiO<sub>2</sub> calcined in argon atmosphere, *Appl. Surf. Sci.* 430 (2018) 407–414, <https://doi.org/10.1016/j.apsusc.2017.08.071>.
- [49] S. Phromma, T. Wutikhun, P. Kasamechonchung, T. Eksangsri, C. Sapcharoenkun, Effect of calcination temperature on photocatalytic activity of synthesized TiO<sub>2</sub> nanoparticles via wet ball milling sol-gel method, *Appl. Sci.* 10 (3) (2020), <https://doi.org/10.3390/app10030993>.
- [50] A.W. Morawski, et al., Influence of the calcination of TiO<sub>2</sub>-reduced graphite hybrid for the photocatalytic reduction of carbon dioxide, *Catal. Today* 380 (May) (2021) 32–40, <https://doi.org/10.1016/j.cattod.2021.05.017>.
- [51] A.A. Khan, M. Tahir, Recent advancements in engineering approach towards design of photo-reactors for selective photocatalytic CO<sub>2</sub> reduction to renewable fuels, *J. CO<sub>2</sub> Util.* 29 (2018) 205–239, <https://doi.org/10.1016/j.jcou.2018.12.008>, May 2018.
- [52] S. Ali, et al., Gas phase photocatalytic CO<sub>2</sub> reduction, 'a brief overview for benchmarking, *Catalysts* 9 (9) (2019) 1–26, <https://doi.org/10.3390/catal9090727>.
- [53] M. Dilla, A.E. Becerikli, A. Jakubowski, R. Schlögl, S. Ristig, Development of a tubular continuous flow reactor for the investigation of improved gas-solid interaction in photocatalytic CO<sub>2</sub> reduction on TiO<sub>2</sub>, *Photochem. Photobiol. Sci.* 18 (2) (2019) 314–318, <https://doi.org/10.1039/c8pp00518d>.
- [54] M. Tahir, Enhanced photocatalytic CO<sub>2</sub> reduction to fuels through bireforming of methane over structured 3D MAX Ti<sub>3</sub>AlC<sub>2</sub>/TiO<sub>2</sub> heterojunction in a monolith photoreactor, *J. CO<sub>2</sub> Util.* 38 (2020) 99–112, <https://doi.org/10.1016/j.jcou.2020.01.009>, January.
- [55] D. Giusti, C. Ampelli, C. Genovese, S. Perathoner, G. Centi, A novel gas flow-through photocatalytic reactor based on copper-functionalized nanomembranes for the photoreduction of CO<sub>2</sub> to C1-C2 carboxylic acids and C1-C3 alcohols, *Chem. Eng. J.* 408 (2021), 127250, <https://doi.org/10.1016/j.cej.2020.127250>, July 2020.
- [56] J. Cai, F. Shen, Z. Shi, Y. Lai, J. Sun, Nanostructured TiO<sub>2</sub> for light-driven CO<sub>2</sub> conversion into solar fuels, *Appl. Mater.* 8 (4) (2020), <https://doi.org/10.1063/1.5144106>.
- [57] X. Zhang, G. Zhang, C. Song, X. Guo, Catalytic conversion of carbon dioxide to methanol: current status and future perspective, *Front. Energy Res.* 8 (2021) 1–16, <https://doi.org/10.3389/fenrg.2020.621119>, February.
- [58] A. Durga Devi, S. Pushpavanam, N. Singh, J. Verma, M.P. Kaur, S.C. Roy, Enhanced methane yield by photoreduction of CO<sub>2</sub> at moderate temperature and pressure using Pt coated, graphene oxide wrapped TiO<sub>2</sub> nanotubes, *Results Eng* 14 (2022), 100441, <https://doi.org/10.1016/j.rineng.2022.100441>, February.
- [59] F.F. Patricia Reñones, Laura Collado, Ana Iglesias-Juez, Freddy E. Oropeza, V.A. de la P. O'Shea, Silver-gold bimetal-loaded TiO<sub>2</sub> photocatalysts for CO<sub>2</sub> reduction, *Ind. Eng. Chem. Res.* 59 (20) (2020) 9440–9450, <https://doi.org/10.1021/acs.iecr.0c01034>.
- [60] A. Sanz-Marco, et al., LED-driven controlled deposition of Ni onto TiO<sub>2</sub> for visible-light expanded conversion of carbon dioxide into C1-C2 alkanes, *Nanoscale Adv.* 3 (13) (2021) 3788–3798, <https://doi.org/10.1039/d1na00021g>.
- [61] M. Liu, et al., Substrate-dependent ALD of Cux on TiO<sub>2</sub> and its performance in photocatalytic CO<sub>2</sub> reduction, *Chem. Eng. J.* 405 (2021), 126654, <https://doi.org/10.1016/j.cej.2020.126654>, August 2020.
- [62] Z. Zhan, et al., Grafting hypercrosslinked polymers on TiO<sub>2</sub> surface for anchoring ultrafine Pd nanoparticles: dramatically enhanced efficiency and selectivity toward photocatalytic reduction of CO<sub>2</sub> to CH<sub>4</sub>, *Small* 18 (1) (2022), <https://doi.org/10.1002/sml.202105083>.
- [63] X. Feng, F. Pan, B.Z. Tran, Y. Li, Photocatalytic CO<sub>2</sub> reduction on porous TiO<sub>2</sub> synergistically promoted by atomic layer deposited MgO overcoating and photodeposited silver nanoparticles, *Catal. Today* 339 (2020) 328–336, <https://doi.org/10.1016/j.cattod.2019.03.012>, March 2019.
- [64] F. Khatun, A. Abd Aziz, L.C. Sim, M.U. Monir, Plasmonic enhanced Au decorated TiO<sub>2</sub> nanotube arrays as a visible light active catalyst towards photocatalytic CO<sub>2</sub> conversion to CH<sub>4</sub>, *J. Environ. Chem. Eng.* 7 (6) (2019), 103233, <https://doi.org/10.1016/j.jece.2019.103233>.
- [65] Y. Li, C. Wang, M. Song, D. Li, X. Zhang, Y. Liu, TiO<sub>2-x</sub>/CoO<sub>x</sub> photocatalyst sparks in photothermocatalytic reduction of CO<sub>2</sub> with H<sub>2</sub>O steam, *Appl. Catal. B Environ.* 243 (2019) 760–770, <https://doi.org/10.1016/j.apcatb.2018.11.022>, October 2018.
- [66] M. Ijaz, M. Zafar, Titanium dioxide nanostructures as efficient photocatalyst: progress, challenges and perspective, *Int. J. Energy Res.* 45 (3) (2021) 3569–3589, <https://doi.org/10.1002/er.6079>.
- [67] R. Nematollahi, C. Ghotbi, F. Khorasheh, A. Larimi, Ni-Bi co-doped TiO<sub>2</sub> as highly visible light response nano-photocatalyst for CO<sub>2</sub> photo-reduction in a batch

- photo-reactor, *J. CO<sub>2</sub> Util.* 41 (August) (2020), 101289, <https://doi.org/10.1016/j.jcou.2020.101289>.
- [68] R.S. Pedaneekar, S.K. Shaikh, K.Y. Rajpure, Thin film photocatalysis for environmental remediation: a status review, *Curr. Appl. Phys.* 20 (8) (2020) 931–952, <https://doi.org/10.1016/j.cap.2020.04.006>.
- [69] Y. Wei, et al., Efficient photocatalysts of TiO<sub>2</sub> nanocrystals-supported PtRu alloy nanoparticles for CO<sub>2</sub> reduction with H<sub>2</sub>O: synergistic effect of Pt-Ru, *Appl. Catal. B Environ.* 236 (2018) 445–457, <https://doi.org/10.1016/j.apcatb.2018.05.043>, February.
- [70] M. Tahir, Photocatalytic carbon dioxide reduction to fuels in continuous flow monolith photoreactor using montmorillonite dispersed Fe/TiO<sub>2</sub> nanocatalyst, *J. Clean. Prod.* 170 (2018) 242–250, <https://doi.org/10.1016/j.jclepro.2017.09.118>.
- [71] L. Collado, et al., Unravelling the effect of charge dynamics at the plasmonic metal/semiconductor interface for CO<sub>2</sub> photoreduction, *Nat. Commun.* 9 (1) (2018) 1–10, <https://doi.org/10.1038/s41467-018-07397-2>.
- [72] M. Zhu, Q. Ge, X. Zhu, Catalytic reduction of CO<sub>2</sub> to CO via reverse water gas shift reaction: recent advances in the design of active and selective supported metal catalysts, *Trans. Tianjin Univ.* 26 (3) (2020) 172–187, <https://doi.org/10.1007/s12209-020-00246-8>.
- [73] A. Hammad, et al., Photodeposition conditions of silver cocatalyst on titanium oxide photocatalyst directing product selectivity in photocatalytic reduction of carbon dioxide with water, *Catal. Lett.* 150 (4) (2020) 1081–1088, <https://doi.org/10.1007/s10562-019-02997-z>.
- [74] H. Pan, X. Wang, Z. Xiong, M. Sun, M. Murugananthan, Y. Zhang, Enhanced photocatalytic CO<sub>2</sub> reduction with defective TiO<sub>2</sub> nanotubes modified by single-atom binary metal components, *Environ. Res.* 198 (April) (2021), 111176, <https://doi.org/10.1016/j.envres.2021.111176>.
- [75] L. Jin, et al., Surface basicity of metal@TiO<sub>2</sub> to enhance photocatalytic efficiency for CO<sub>2</sub> reduction, *ACS Appl. Mater. Interfaces* 13 (32) (2021) 38595–38603, <https://doi.org/10.1021/acsami.1c09119>.
- [76] K. Wang, J. Lu, Y. Lu, C.H. Lau, Y. Zheng, X. Fan, Unravelling the C–C coupling in CO<sub>2</sub> photocatalytic reduction with H<sub>2</sub>O on Au/TiO<sub>2-x</sub>: combination of plasmonic excitation and oxygen vacancy, *Appl. Catal. B Environ.* 292 (2021), 120147, <https://doi.org/10.1016/j.apcatb.2021.120147>, March.
- [77] Y. Zhou, Q. Zhang, X. Shi, Q. Song, C. Zhou, D. Jiang, Photocatalytic reduction of CO<sub>2</sub> into CH<sub>4</sub> over Ru-doped TiO<sub>2</sub>: synergy of Ru and oxygen vacancies, *J. Colloid Interface Sci.* 608 (2022) 2809–2819, <https://doi.org/10.1016/j.jcis.2021.11.011>.
- [78] D. Adekoya, M. Tahir, N.A.S. Amin, Recent trends in photocatalytic materials for reduction of carbon dioxide to methanol, *Renew. Sustain. Energy Rev.* 116 (September) (2019), 109389, <https://doi.org/10.1016/j.rser.2019.109389>.
- [79] N.U.M. Nor, N.A.S. Amin, Glucose precursor carbon-doped TiO<sub>2</sub> heterojunctions for enhanced efficiency in photocatalytic reduction of carbon dioxide to methanol, *J. CO<sub>2</sub> Util.* 33 (2019) 372–383, <https://doi.org/10.1016/j.jcou.2019.07.002>, June.
- [80] A. Bjelajac, et al., Micro-kinetic modelling of photocatalytic CO<sub>2</sub> reduction over undoped and N-doped TiO<sub>2</sub>, *Catal. Sci. Technol.* 10 (6) (2020) 1688–1698, <https://doi.org/10.1039/c9cy02443c>.
- [81] M.H. Foghani, O. Tavakoli, M.J. Parnian, R. Zarghami, Enhanced visible light photocatalytic CO<sub>2</sub> reduction over direct Z-scheme heterojunction Cu/P co-doped g-C<sub>3</sub>N<sub>4</sub>@TiO<sub>2</sub> photocatalyst, *Chem. Pap.* 76 (6) (2022) 3459–3469, <https://doi.org/10.1007/s11696-022-02109-z>.
- [82] C. Thamaraiselvan, et al., Laser-induced graphene and carbon nanotubes as conductive carbon-based materials in environmental technology, *Mater. Today* 34 (April) (2020) 115–131, <https://doi.org/10.1016/j.mattod.2019.08.014>.
- [83] S. Ali, A. Razaq, S. Il, Development of graphene based photocatalysts for CO<sub>2</sub> reduction to C1 chemicals: a brief overview, *Catal. Today* 335 (2019) 39–54, <https://doi.org/10.1016/j.cattod.2018.12.003>, December 2018.
- [84] Y. Lu, Z.A. Khan, M.S. Alvarez-Alvarado, Y. Zhang, Z. Huang, M. Imran, A critical review of sustainable energy policies for the promotion of renewable energy sources, *Sustain. Times* 12 (12) (2020) 1–30, <https://doi.org/10.3390/su12125078>.
- [85] Y. Yang, et al., Double-sided modification of TiO<sub>2</sub> spherical shell by graphene sheets with enhanced photocatalytic activity for CO<sub>2</sub> reduction, *Appl. Surf. Sci.* 537 (2021), 147991, <https://doi.org/10.1016/j.apsusc.2020.147991>, October 2020.
- [86] J.O. Olowoyo, et al., Self-assembled reduced graphene oxide-TiO<sub>2</sub> nanocomposites: synthesis, DFTB+ calculations, and enhanced photocatalytic reduction of CO<sub>2</sub> to methanol, *Carbon N. Y.* 147 (2019) 385–397, <https://doi.org/10.1016/j.carbon.2019.03.019>.
- [87] J. Fernández-Catalá, M. Navlani-García, Berenguer-Murcia, and D. Cazorla-Amorós, “Exploring CuxO-doped TiO<sub>2</sub> modified with carbon nanotubes for CO<sub>2</sub> photoreduction in a 2D-flow reactor,” *J. CO<sub>2</sub> Util.*, vol. 54, 2021, doi: 10.1016/j.jcou.2021.101796.
- [88] F. Khatun, A.A. Aziz, L.C. Sim, Preparation of reduced graphene oxide (RGO) modified titanium dioxide nanotube (TNTs) as visible light effective catalyst for the conversion of CO<sub>2</sub> to CH<sub>4</sub>, *IONP Conf. Ser. Mater. Sci. Eng.* 736 (4) (2020), <https://doi.org/10.1088/1757-899X/736/4/042002>.
- [89] J. Zhang, J. Xu, F. Tao, Interface modification of TiO<sub>2</sub> nanotubes by biomass-derived carbon quantum dots for enhanced photocatalytic reduction of CO<sub>2</sub>, *ACS Appl. Energy Mater.* 4 (11) (2021) 13120–13131, <https://doi.org/10.1021/acsaelm.1c02760>.
- [90] S. Liu, T. Jiang, M. Fan, G. Tan, S. Cui, and X. Shen, “Nanostructure rod-like TiO<sub>2</sub>-reduced graphene oxide composite aerogels for highly-efficient visible-light photocatalytic CO<sub>2</sub> reduction,” *J. Alloys Compd.*, vol. 861, 2021, doi: 10.1016/j.jallcom.2021.158598.
- [91] R. Goutham, R. Badri Narayan, B. Srikanth, K.P. Gopinath, Supporting Materials for Immobilisation of Nano-Photocatalysts, 2019, pp. 49–82, [https://doi.org/10.1007/978-3-030-10609-6\\_2](https://doi.org/10.1007/978-3-030-10609-6_2).
- [92] M. Tasbihi, et al., On the selectivity of CO<sub>2</sub> photoreduction towards CH<sub>4</sub> using Pt/TiO<sub>2</sub> catalysts supported on mesoporous silica, *Appl. Catal. B Environ.* 239 (2018) 68–76, <https://doi.org/10.1016/j.apcatb.2018.08.003>, July.
- [93] A. Larimi, M.R. Rahimi, F. Khorasheh, Carbonaceous supports decorated with Pt-TiO<sub>2</sub> nanoparticles using electrostatic self-assembly method as a highly visible-light active photocatalyst for CO<sub>2</sub> photoreduction, *Renew. Energy* 145 (2020) 1862–1869, <https://doi.org/10.1016/j.renene.2019.07.105>.
- [94] Y. Ku, P.C. Lee, G.K. Luong, Photocatalytic reduction of gaseous carbon dioxide over NiO/TiO<sub>2</sub> under UV light illumination, *J. Taiwan Inst. Chem. Eng.* 125 (2021) 291–296, <https://doi.org/10.1016/j.jtice.2021.06.036>.
- [95] H. Rao, C.H. Lim, J. Bonin, G.M. Miyake, M. Robert, Visible-light-driven conversion of CO<sub>2</sub> to CH<sub>4</sub> with an organic sensitizer and an iron porphyrin catalyst, *J. Am. Chem. Soc.* 140 (51) (2018) 17830–17834, <https://doi.org/10.1021/jacs.8b09740>.
- [96] M. Jo, et al., Utility of squaraine dyes for dye-sensitized photocatalysis on water or carbon dioxide reduction, *ACS Omega* 4 (10) (2019) 14272–14283, <https://doi.org/10.1021/acsomega.9b01914>.
- [97] M. Cheng, S. Bai, Y. Xia, X. Zhu, R. Chen, Q. Liao, Highly efficient photocatalytic conversion of gas phase CO<sub>2</sub> by TiO<sub>2</sub> nanotube array sensitized with CdS/ZnS quantum dots under visible light, *Int. J. Hydrogen Energy* 46 (62) (2021) 31634–31646, <https://doi.org/10.1016/j.ijhydene.2021.07.067>.
- [98] B. Chon, S. Choi, Y. Seo, H.S. Lee, C.H. Kim, H. Son, InP-Quantum Dot Surface-Modified TiO<sub>2</sub> Catalysts for Sustainable Photochemical Carbon Dioxide Reduction, 2022, <https://doi.org/10.1021/acscuchemeng.2c00938>.
- [99] Q. Chen, et al., Activation of molecular oxygen in selectively photocatalytic organic conversion upon defective TiO<sub>2</sub> nanosheets with boosted separation of charge carriers, *Appl. Catal. B Environ.* 262 (2020), 118258, <https://doi.org/10.1016/j.apcatb.2019.118258>, September 2019.
- [100] P. Seeharaj, et al., Ultrasonically-assisted surface modified TiO<sub>2</sub>/rGO/CeO<sub>2</sub> heterojunction photocatalysts for conversion of CO<sub>2</sub> to methanol and ethanol, *Ultrason. Sonochem.* 58 (2019), <https://doi.org/10.1016/j.ultrsonch.2019.104657>, May.
- [101] F. Xu, H. Tan, J. Fan, B. Cheng, J. Yu, J. Xu, Electrospun TiO<sub>2</sub>-based photocatalysts, *Sol. RRL* 5 (6) (2021) 1–28, <https://doi.org/10.1002/solr.202000571>.
- [102] B.T. Barrocas, N. Ambrožová, K. Kočí, Photocatalytic reduction of carbon dioxide on TiO<sub>2</sub> heterojunction photocatalysts—a review, *Sol. Energy Convers. Storage Photochem. Modes* 15 (967) (2022) 173–185, <https://doi.org/10.3390/ma15030967>.
- [103] H. Wang, et al., TiO<sub>2</sub> modified g-C<sub>3</sub>N<sub>4</sub> with enhanced photocatalytic CO<sub>2</sub> reduction performance, *Solid State Sci.* 100 (2020), 106099, <https://doi.org/10.1016/j.solidstatesciences.2019.106099>, October 2019.
- [104] F. Zhang, et al., Photothermal catalytic CO<sub>2</sub> reduction over nanomaterials, *Chem Catal* 1 (2) (2021) 272–297, <https://doi.org/10.1016/j.cheecat.2021.01.003>.
- [105] K. M. Kamal et al., “Synergistic enhancement of photocatalytic CO<sub>2</sub> reduction by plasmonic Au nanoparticles on TiO<sub>2</sub> decorated N-graphene heterostructure catalyst for high selectivity methane production,” *Appl. Catal. B Environ.*, vol. 307, 2022, doi: 10.1016/j.apcatb.2022.121181.
- [106] Q. Xu, L. Zhang, B. Cheng, J. Fan, J. Yu, S-scheme heterojunction photocatalyst, *Chem* 6 (7) (2020) 1543–1559, <https://doi.org/10.1016/j.chempr.2020.06.010>.
- [107] M. Tahir, B. Tahir, Constructing S-scheme 2D/0D g-C<sub>3</sub>N<sub>4</sub>/TiO<sub>2</sub> NPs/MPs heterojunction with 2D-Ti<sub>3</sub>AlC<sub>2</sub> MAX cocatalyst for photocatalytic CO<sub>2</sub> reduction to CO/CH<sub>4</sub> in fixed-bed and monolith photoreactors, *J. Mater. Sci. Technol.* 106 (2022) 195–210, <https://doi.org/10.1016/j.jmst.2021.08.019>.
- [108] X. Wang, et al., BiVO<sub>4</sub>/Bi<sub>4</sub>Ti<sub>3</sub>O<sub>12</sub> heterojunction enabling efficient photocatalytic reduction of CO<sub>2</sub> with H<sub>2</sub>O to CH<sub>3</sub>OH and CO, *Appl. Catal. B Environ.* 270 (2020), <https://doi.org/10.1016/j.apcatb.2020.118876>, March.
- [109] G. Huang, et al., Preparation of an In<sub>2</sub>S<sub>3</sub>/TiO<sub>2</sub> heterostructure for enhanced activity in carbon dioxide photocatalytic reduction, *ChemPhotoChem* 5 (5) (2021) 438–444, <https://doi.org/10.1002/cptc.202000295>.
- [110] X. Wu, et al., Multifunctional photocatalysts of Pt-decorated 3DOM perovskite-type SrTiO<sub>3</sub> with enhanced CO<sub>2</sub> adsorption and photoelectron enrichment for selective CO<sub>2</sub> reduction with H<sub>2</sub>O to CH<sub>4</sub>, *J. Catal.* 377 (2019) 309–321, <https://doi.org/10.1016/j.jcat.2019.07.037>.
- [111] A. Han, et al., Ti<sup>3+</sup> defective SnS<sub>2</sub>/TiO<sub>2</sub> heterojunction photocatalyst for visible-light driven reduction of CO<sub>2</sub> to CO with high selectivity, *Catalysts* 9 (2019) 11, <https://doi.org/10.3390/catal9110927>.
- [112] M. Tahir, Well-designed ZnFe<sub>2</sub>O<sub>4</sub>/Ag/TiO<sub>2</sub> nanorods heterojunction with Ag as electron mediator for photocatalytic CO<sub>2</sub> reduction to fuels under UV/visible light, *J. CO<sub>2</sub> Util.* 37 (2020) 134–146, <https://doi.org/10.1016/j.jcou.2019.12.004>, November 2019.
- [113] F. Hasanvandian, M. Zehtab Salmasi, M. Moradi, S. Farshineh Saei, B. Kakavandi, S. Rahman Setayesh, Enhanced spatially coupling heterojunction assembled from CuCo<sub>2</sub>S<sub>4</sub> yolk-shell hollow sphere encapsulated by Bi-modified TiO<sub>2</sub> for highly

- efficient CO<sub>2</sub> photoreduction, Chem. Eng. J. 444 (April) (2022), 136493, <https://doi.org/10.1016/j.cej.2022.136493>.
- [114] Z. Wang, Y. Chen, L. Zhang, B. Cheng, J. Yu, J. Fan, Step-scheme CdS/TiO<sub>2</sub> nanocomposite hollow microsphere with enhanced photocatalytic CO<sub>2</sub> reduction activity, J. Mater. Sci. Technol. 56 (2020) 143–150, <https://doi.org/10.1016/j.jmst.2020.02.062>.
- [115] Z. Dong, Z. Zhang, Y. Jiang, Y. Chu, J. Xu, Embedding CsPbBr<sub>3</sub> perovskite quantum dots into mesoporous TiO<sub>2</sub> beads as an S-scheme heterojunction for CO<sub>2</sub> photoreduction, Chem. Eng. J. 433 (P3) (2022), 133762, <https://doi.org/10.1016/j.cej.2021.133762>.